https://doi.org/10.5194/bg-2022-69
Preprint. Discussion started: 6 April 2022

Biogeosciences Discussions

Meteorological responses of carbon dioxide and methane fluxes in the terrestrial and aquatic ecosystems of a subarctic landscape

Lauri Heiskanen[1], Juha-Pekka Tuovinen[1], Aleksi Räsänen[2,3], Tarmo Virtanen[2], Sari Juutinen[2,4], Henriikka Vekuri[1], Annalea Lohila[1], Juha Mikola[2,3], Mika Aurela[1]

[1]Climate System Research Unit, Finnish Meteorological Institute, Helsinki, Finland
[2]Ecosystems and Environment Research Programme, Faculty of Biological and Environmental Sciences, University of Helsinki, Helsinki, Finland
[3]Natural Resources Institute Finland (LUKE), Helsinki, Finland
[4]University of Eastern Finland, Department of Geographical and Historical Studies, Joensuu, Finland

Correspondence to: Lauri Heiskanen (lauri.heiskanen@fmi.fi)

Abstract

The subarctic landscape consists of a mosaic of forest, peatland and aquatic ecosystems and their ecotones. The carbon (C) exchange between ecosystems and the atmosphere through carbon dioxide (CO_2) and methane (CH_4) fluxes varies spatially and temporally among these ecosystems. Our study area in Kaamanen in northern Finland covered 7 km^2 of boreal subarctic landscape with upland forest, open peatland, pine bogs and lakes. We measured the CO_2 and CH_4 fluxes with eddy covariance and chambers between June 2017 and June 2019 and studied the C flux responses to varying meteorological conditions. The landscape area was an annual CO_2 sink of -25.9 ± 65.7 and -41.3 ± 64.9 g C m^{-2}, and a CH_4 source of 2.4 ± 0.7 and 2.3 ± 0.7 g C m^{-2} during the first and second study year, respectively. The pine forest had the largest contribution to the landscape-level CO_2 sink, -78.3 ± 50.8 and -118.9 ± 26.8 g C m^{-2}, and the fen to the CH_4 emissions, 7.0 ± 0.2 and 6.3 ± 0.3 g C m^{-2}, during the first and second study year, respectively. The lakes within the area acted as CO_2 and CH_4 sources to the atmosphere throughout the measurement period, with an organic sediment lake located downstream from the fen showing sixfold fluxes compared to a mineral sediment lake. The annual C balances were affected most by the rainy peak growing season of 2017 and the heatwave and drought event in July 2018. The rainy period increased the ecosystem respiration of the pine forest due to continuously high soil moisture content. A similar flux response to abundant precipitation was not observed for the fen ecosystem, which is adapted to high water table levels. During the heatwave and drought period, similar responses were observed for all terrestrial ecosystems, with decreased gross primary productivity and net CO_2 uptake, caused by the unfavourable growing conditions and plant stress due to the soil moisture and vapour pressure deficits. Additionally, the CH_4 emissions from the fen decreased during and after the drought. However, the timing and duration of drought effects varied between fen and forest ecosystems, as C fluxes were affected sooner and had a shorter post-drought recovery time in the fen than forests. The differing CO_2 flux response to weather variations showed that terrestrial ecosystems can have a contrasting impact on the landscape-level C balance in a changing climate, even if they function similarly most of the time.

https://doi.org/10.5194/bg-2022-69
Preprint. Discussion started: 6 April 2022

1 Introduction

A typical boreal subarctic landscape consists of a mosaic of land cover types including forests, open and forested peatlands and water bodies, with each ecosystem acting as a source or sink of atmospheric carbon (C) depending on its characteristics and weather conditions. To grasp a full picture of the C balance at the landscape scale, the carbon dioxide (CO_2) and methane (CH_4) exchange between the main ecosystems and the atmosphere needs to be assessed. This is also because part of the C fixed in terrestrial systems can be emitted back to the atmosphere via aquatic ecosystems or transported out from the catchment. The net atmosphere-ecosystem CO_2 exchange is a result of gross primary production (GPP) of plants and ecosystem respiration (ER), which is composed of autotrophic and heterotrophic respiration (Chapin et al., 2011). The CH_4 emissions from ecosystems are mainly produced by methanogens in the waterlogged anaerobic zone in soils, while the CH_4 uptake is caused by oxidation by methanotrophs in aerobic soil conditions (Le Mer and Roger, 2001).

As a result of the ongoing climate change, the subarctic regions warm rapidly, two to three times as fast as the rest of the world (Masson-Delmotte et al., 2018). The higher temperatures affect the C cycle of subarctic ecosystems by lengthening the growing season and shortening the snow and ice cover periods. Higher temperatures and a longer growing season enable greater CO_2 uptake through photosynthesis (Aurela et al., 2004; Silfver et al., 2020), but they also allow greater CO_2 emissions due to the increased heterotrophic and autotrophic respiration (Kätterer et al., 1998). However, the variation in ecosystem C dynamics is also highly dependent on water balance, as too low a moisture content in soils decreases GPP and decomposition of organic matter (Jones, 2013; Meyer et al., 2018), and methanogenesis requires anoxic soil conditions (Chapin et al., 2011). In aquatic ecosystems, the longer ice-free periods, with increased C input from surrounding terrestrial ecosystems, lead to higher annual C emissions to the atmosphere (Cole et al., 2007, Guo et al., 2020). In a longer than one-year timespan, the effects of climate change are observed as vegetation composition shifts, such as Arctic shrubification that enhances CO_2 uptake and alters ecosystem respiration and nutrient availability (Mekonnen et al., 2021). Concurrently, the potential of severe weather events, such as heatwaves and droughts, to affect the C cycles increases within the region (Masson-Delmotte et al., 2018).

Boreal upland forests have been shown to act as either annual net sinks or sources of atmospheric CO_2, depending on species composition, climatic conditions and the occurrence of extreme weather events, fires, and herbivories and pathogens (Bond-Lamberty et al., 2007; Kljun et al., 2007; Lindroth et al., 2008; Aurela et al., 2015; Hadden and Grelle, 2017), and these ecosystems usually act as small CH_4 sinks (Dinsmore et al., 2017). Undrained boreal peatlands have been, in a long term, net CO_2 sinks via accumulation of organic C, but similarly to forests their annual CO_2 balance is sensitive to environmental conditions (Bubier et al., 1998; Aurela et al., 2004; Lindroth et al., 2007). Additionally, these peatlands release CH_4 into the atmosphere (Chapin et al., 2011). Peatlands have more C stored in the soil, but less C in living plant matter compared to upland forests, and thus the same disturbances on the ecosystems can lead to differing effects on the C balance.

Globally, inland waters act as net CO_2 and CH_4 sources to the atmosphere (Tranvik et al., 2009). Boreal lakes vary greatly in their area and depth, input of organic and inorganic C from the terrestrial ecosystems, ice-free period duration and the amount of C in sediments and aquatic vegetation, which all affect the magnitude of the C exchange with the atmosphere (Bastviken et

https://doi.org/10.5194/bg-2022-69
Preprint. Discussion started: 6 April 2022

al., 2004; Wik et al., 2018; Denfeld et al., 2020). Additionally, water bodies provide paths for lateral flow of water, C and other matter between ecosystems (Cole et al., 2007).

The landscape-level C balance comprised of diverse ecosystems is evidently dependent on the ecosystem composition, and the regional effect of an environmental change or disturbance depends on the integrated response of individual ecosystems. As an example of such a disturbance, a heatwave and drought event encompassed north-western Europe during the summer of 2018 (Lehtonen and Pirinen, 2019 a, b). The drought conditions had different effects on the CO_2 exchange of boreal forests and peatlands in the area (Rinne et al., 2020; Lindroth et al., 2020; Matkala et al., 2021). There was large variation in how different forests reacted to the heatwave and drought, some showing a substantial decrease and some no change or even an increase in CO_2 uptake (Lindroth et al., 2020; Matkala et al., 2021). Most of the studied peatlands turned momentarily into CO_2 sources during the drought, which lowered their annual CO_2 uptake significantly, and simultaneously the CH_4 emissions decreased (Rinne et al., 2020). Thus, the landscape-level C balance depends on multiple responses, whose net effect are not easily predictable.

In this study, we assess the ecosystem-atmosphere exchange of CO_2 and CH_4 within a subarctic landscape based on eddy covariance and chamber measurements. The studied area in Kaamanen in northern Finland include an upland pine forest, pine bogs, a mesotrophic flark fen and shallow lakes of glacial origin. We focus on the temporal variation of C exchange during two full years (June 2017 – June 2019). The meteorological conditions during the first year were similar to the long-term average, with the exception of the higher-than-average precipitation sum in summer. The second year included the above-mentioned heatwave and drought period. Motivated by the plant community-level study of Heiskanen et al. (2021), who found that the diversity of plant communities constrained C loss from the Kaamanen fen during the 2018 drought, we study if a similar pattern can be observed at the ecosystem level.

Here, we address questions how sensitive the C fluxes of different ecosystems are to changes in environmental conditions and how this is reflected on the landscape-level C exchange. The more specific scientific questions addressed are: (1) What are the contributions of each ecosystem to the landscape-level CO_2 and CH_4 fluxes? (2) Do the CO_2 and CH_4 fluxes of different ecosystems show similar responses to varying meteorological conditions?

2 Materials and methods

2.1 Study site

The studied landscape is in Kaamanen in northern Finland (69°8' N, 27°16' E; 155 m a.s.l.) within the subarctic climate zone and the northern boreal vegetation zone. The annual mean temperature in the region was -0.4 °C and the mean annual precipitation sum 472 mm in 1981–2010 (Pirinen et al., 2012). Even though the study area is located within the sporadic permafrost zone, no permafrost has been found there anymore in recent decades (Fronzek et al., 2010). The growing season is short and lasts for 150–180 days (Aurela et al., 2002). The study area covers 7 km^2 around the flux measurement sites (Fig. 1) and consists of five main ecosystem types: upland pine forest, patterned mesotrophic flark fen, treed pine bog, sparsely treed

https://doi.org/10.5194/bg-2022-69
Preprint. Discussion started: 6 April 2022

Biogeosciences Discussions

pine bog, and lakes and a connecting stream (Fig. 2). The ecosystems within the study area are homogeneous in their species composition and provide a representative sample of the landscape.

The areal coverage of different ecosystem types in the landscape was estimated with a land cover classification utilizing remote sensing data and field observations following the methodology described by Räsänen and Virtanen (2019). An aerial orthophoto was segmented, 55 features for each segment were calculated from multi-source remote sensing data, including orthophoto, aerial laser scanning and satellite imagery, and a supervised random forest classification (Breiman 2001) was carried out using field data for model training and validation (Supplement S.1). The pine forest, pine bog, fen and lake ecosystems each encompass roughly an equal area (Table 1). The ecosystems in the area are pristine with the exception of some forest loggings, thinning and selective removal of birches in part of the pine-dominated forests.

The mesotrophic flark fen is an open peatland ecosystem characterised by a mosaic of string and flark microforms, with the 0.5–1 m high string formations can remain frozen until the late summer (Aurela et al., 2001). The fen has a clear patterning and can be partitioned to five distinct plant community types (PCTs) that differ in their vegetation composition, water table level and carbon fluxes (Maanavilja et al., 2011; Räsänen et al. 2019; Heiskanen et al., 2021). In the flarks, the plant communities are dominated by sedges, including *Trichophorum* tussocks, and brown mosses. The top of the strings act as ombrotrophic bog surfaces within the fen and are covered mainly by dwarf shrubs, herbs, mosses and lichens, while string margins are populated by dwarf birch (*Betula nana)* and other dwarf shrubs, sedges and *Sphagnum* mosses. The fifth PCT, a tall sedge fen that is covered by tall sedges, deciduous shrubs and forbs, can be found in the riparian areas of lakes and small streams. The species composition of these PCTs was described in detail by Maanavilja et al. (2011) and Räsänen et al. (2019), and paleorecords by Piilo et al. (2020). The bedrock under the peatland slopes towards the south. The average peat thickness increases from 1 m in the northern part of the fen towards the south, where it is up to 4 m (Piilo et al., 2020). Most of the aboveground biomass of the peatland resides in shrubs and mosses, and forbs and graminoids contribute increasingly to the total leaf area in the mid and late growing season (Table A1).

The dominant tree species in the upland mineral soil forest is Scots pine (*Pinus sylvestris*) with a few downy birch (*Betula pubescens*) trees also present. The forest around the flux measurement site was logged about 50 yr ago, but most of the pine forests within the study area are pine-dominated old-growth forest with an uneven age distribution. The average height of all trees and the main canopy were approximately 8 and 11 m, respectively (Table A2). The field layer is dominated by evergreen dwarf shrubs (e.g. *Vaccinium vitis-idaea* and *Calluna vulgaris*), and the ground layer is covered by mosses and lichens. The soil type in the forest is sandy podzol, which has higher bulk density, lower N content and higher C:N ratio than the soil in the peatlands (Table A3). Mosses and lichens contribute about 10 % to the total aboveground biomass (Table A1).

The tree height and density decrease from the upland pine forest to the pine bog ecosystems. The average tree height in the pine bog was 5 m, and in treed pine bog and sparsely treed pine bog the above-ground tree biomass was about 50 % and 16 %, respectively, of the biomass in pine forest (Tables A2, A4). The field layer vegetation of the pine bog ecosystems is similar to that of the string tops (Table A1), with evergreen (*Ledum palustre*) and deciduous (*Vaccinium uliginosum* and *Betula nana*) shrubs, herbs (*Rubus chamaemorus*) and graminoids (mostly *Carex* spp.). The pine bog ground layer is formed by mosses and

https://doi.org/10.5194/bg-2022-69
Preprint. Discussion started: 6 April 2022

a few lichens. The soil carbon content is higher in the sparsely treed bog patches within the fen than in bog vegetation with thinner organic layer at the forest edge. Soil N content and C:N ratio are similar to those found in pine forest and string tops (Table A3).

The water bodies within the study area vary in size from small streams and ponds to lakes larger than 25 ha (Lake Ulkujärvi in the northwest and Lake Jänkäjärvi in the south, Fig. 1). The lakes in the area are shallow, the depth ranging from less than 1 m to a few metres and have a sandy or organic sediment bottom. Most water bodies in the study area belong to the same catchment, with water flowing from north to south. The aquatic vegetation is sparse, near the shore consisting of macrophytes, mainly horsetail (*Equisetum fluviatile*), sedges (*Carex* spp.), *Menyanthes trifoliata* and benthic algae. A few-metre-wide stream flows though the peatland and connects Lake Ulkujärvi to Lake Jänkäjärvi. Additionally, water flows on the surface across the fen and through the peat layers and eskers. Each year, during the spring thaw, the fen and partially the pine bogs become flooded.

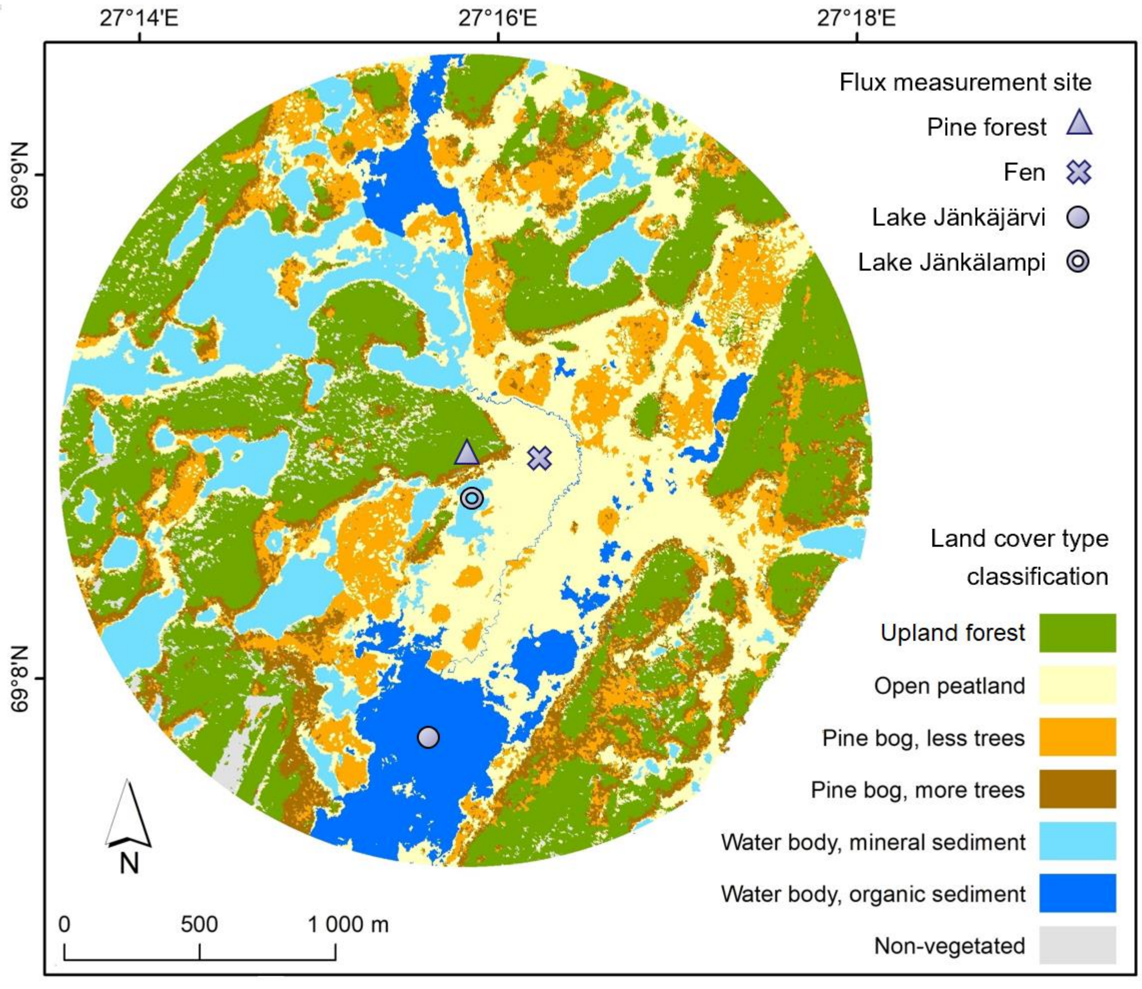

Figure 1. The study area in Kaamanen with land cover type classification and flux measurement site locations.

https://doi.org/10.5194/bg-2022-69
Preprint. Discussion started: 6 April 2022

Biogeosciences
Discussions
Open Access

Table 1. Relative areal coverage of the land cover types within the study area.

Land cover type	Areal coverage [%]
Upland forest	29.2
Pine bog, more trees	9.1
Pine bog, less trees	13.5
Open peatland	26.1
Water body, mineral sediment	12.5
Water body, organic sediment	7.8
Non-vegetated	1.8

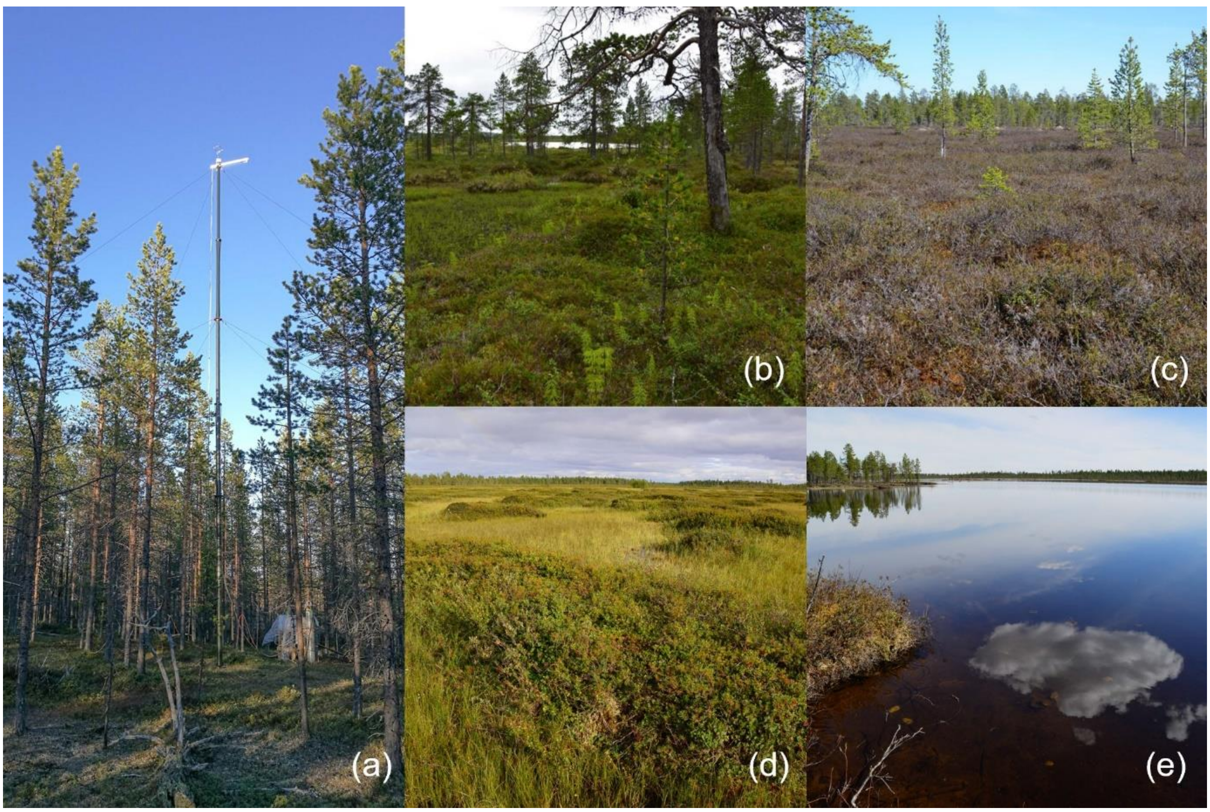

Figure 2. (a) Scots pine forest, (b) treed pine bog, (c) sparsely treed pine bog, (d) fen and (e) lake ecosystems. Photo: (a) Lauri Heiskanen, (b)-(e) Tarmo Virtanen.

2.2 Flux measurement methods

2.2.1 Pine forest flux measurements

The CO_2 flux measurements in the Scots pine forest were set up in the beginning of the growing season in 2017, and data acquisition was started on 8 June 2017. The eddy covariance (EC) measurements were conducted on a 14 m tall tower that was located on the southern edge of the forest so that in the wind sector 250°–65° the forest coverage was higher than 80 %. The EC system consisted of a three-axis sonic anemometer (USA-1, METEK Meteorologische Messtechnik GmbH, Germany) and a closed-path infrared gas analyser for CO_2 and H_2O mixing ratios (LI-7200, LI-COR Biosciences, USA). The inlet tube for the gas analyser was (~18) m long and had an inner tube diameter of (3.1) mm. The flow rate was (5-6) L min^{-1}.

The sampling frequency for the EC flux data was 10 Hz. Standard methods were used for calculating the half-hourly turbulent fluxes (Aubinet et al., 2012), with block averaging and a double rotation of the coordinate system (McMillen, 1988). The high-frequency signal attenuation flux losses were taken into account using an experimental transfer function with a half-power frequency of 1.9 Hz (Laurila et al., 2005).

The half-hourly averaged data were accepted based on the following screening criteria: relative stationarity < 100 % (Foken and Wichura, 1996), number of recorded data per 30 min > 17 400, number of signal spikes per 30 min < 360, mean CO_2 mixing ratio within 340–550 ppm. A friction velocity limit of 0.24 m s^{-1} was used for screening the periods of insufficient turbulence. Data from the wind direction sector 250°–65° were used to calculate the CO_2 balances of the forest.

As the net ecosystem exchange of CO_2 in forests (NEE_{forest}) can be significantly affected by the flux due to storage change below the measurement height, this was estimated according to Montagnani et al. (2018) and added to the measured eddy flux ($F_{\mathrm{CO_2}}$):

$$NEE_{\mathrm{forest}} = F_{\mathrm{CO_2}} + \overline{\rho_d}\frac{\Delta\overline{\mathrm{CO_2}}}{\Delta t}h \quad (1)$$

where $\overline{\rho_d}$ is the mean dry air density, $\frac{\Delta\overline{\mathrm{CO_2}}}{\Delta t}$ is the change of CO_2 dry molar fraction at the EC measurement height during the 30 min averaging period, and h is the measurement height. The CO_2 concentration profile below the measurement height was assumed to be constant.

2.2.2 Fen flux measurements

The CO_2 and CH_4 fluxes of the Kaamanen fen were measured with both the EC and flux chamber methods. The EC measurements were used for the fen ecosystem flux analysis here, and the PCT-specific chamber-based data were used for estimating the CO_2 fluxes of the pine bog ecosystems. Even though the fen is comprised of a mosaic of different PCTs, the contribution of each type is similar in all wind directions within a 100–150 m radius, and thus the footprint variation is not expected to bias the ecosystem balances derived from EC measurements. The measurements were conducted on a 5 m tall tower with a three-axis sonic anemometer (USA-1, METEK Meteorologische Messtechnik GmbH, Germany), a closed-path infrared gas analyser for CO_2 and H_2O mixing ratios (LI-7000, LI-COR Biosciences, USA) and a laser-based gas analyser for

CH_4 mixing ratio (RMT-200, Los Gatos Research, USA). The same flux calculation and data processing methods were used as with the pine forest EC data, except for the discarded wind direction sector (260°–315°) and the friction velocity limit (0.1 m s^{-1}).

The manual chamber measurements of the main plant communities were conducted during the growing season in 2017 and 2018. For modelling the string top CO_2 fluxes for the time span from June 2017 to June 2019, to be used for pine bog (Sect. 2.4), the chamber-based fen ecosystem fluxes were scaled to match the EC-based fen fluxes. This was done similarly to Piilo et al. (2020) by upscaling the chamber fluxes of the main PCTs of the fen to the ecosystem scale according to their relative areas within 200 m from the EC tower (Table 2). The PCT-specific fluxes were presented in more detail by Heiskanen et al. (2021).

Table 2. Area coverage of the plant community types of the peatland inside a 200 m radius around the eddy covariance tower.

Plant community type	Area coverage [%]
Flark	37
Trichophorum tussock	10
Tall sedge fen	17
String margin	14
String top	16
Pine bog	6

The mean ratio between the fen ecosystem-scale chamber-based ER and GPP fluxes and the fen EC fluxes were used for scaling the chamber fluxes calculated from the data measured during the manual chamber measurement days (Table 3). The ER ratio was calculated by using the 24 h data, while the GPP ratio was calculated by using only the daytime data from 6 a.m. to 6 p.m. local standard time.

Table 3. The scaling coefficients used for scaling ER and GPP chamber fluxes.

Time period	ER ratio	GPP ratio
June 2017 – October 2017	1.367	1.620
November 2017 – April 2018	1.142	1.387
May 2018 – June 2019	0.918	1.154

2.2.3 Eddy covariance data gap-filling

The EC flux time series of the pine forest and fen ecosystems had gaps due to equipment failures, wind sector exclusions and quality control filtering applied during the post-processing of data. The gaps in the CO_2 flux data were filled by GPP and ER flux values modelled with environmental response functions, as described by Heiskanen et al. (2021). A rectangular hyperbola was used to model the dependency of GPP on photosynthetic photon flux density (PPFD), while the exponential Lloyd-Taylor

https://doi.org/10.5194/bg-2022-69
Preprint. Discussion started: 6 April 2022

(1994) model was used for ER. For the pine forest flux parameterisation, air temperature was used during the growing season, while soil temperature (T_s) at the 10 cm depth was used for the other periods, while for the fen, T_s at the 10 cm depth was used for the whole year.

The fitting of the GPP function was performed in a moving window with a minimum of 3 days and 30 half-hourly observations of the daytime flux data (PPFD > 30 µmol m^{-2} s^{-1}). For fitting the parameters of the ER function, night-time data were used (PPFD < 30 µmol m^{-2} s^{-1}). The respiration activation energy parameter (E_0) was fitted first with a 91-day moving window, after which the base respiration rate at 10 ºC (R_{10}) was fitted to the data within a moving window of at least 7 days.

A long gap in the pine forest EC flux data in April–June 2019 was filled by utilizing the response function parameters estimated for the same period in 2018. In total, 86 % and 91 % of the forest CO_2 flux data were gap filled in the time series of 11 June 2017 – 10 June 2018 and 11 June 2018 – 10 June 2019, respectively. During the growing seasons, i.e. in 11 June – 31 October 2017 and 11 June – 31 October 2018, the gap-filling percentage was 77 % and 84 %, respectively. The wind direction screening created 43 percentage points of the missing data.

The EC CO_2 fluxes of the fen were gap-filled similarly to the pine forest fluxes. In total, 64 % and 63 % of the fen CO_2 flux data were gap-filled in the time series of the first and second year, respectively. For gap-filling the CH_4 fluxes, a simple moving average interpolation of the half-hour fluxes was used. A moving average window of ± 1, 2, 4, 8, 16 or 32 d was used depending on the length of the gaps in data. In total, 69 % and 70 % of the CH_4 flux data were gap-filled in the time series of the first and second year, respectively.

2.2.4 Lake flux measurements

The diffusive fluxes of CO_2 and CH_4 were measured on the intermediate-side (1.5 ha) mineral sediment Lake Jänkälampi (Fig. 1), hereafter referred to as the MS lake, during the ice-free periods in 2017 and 2018. The diffusive fluxes of these glasses and the CH_4 ebullition flux were measured at the larger, organic sediment Lake Jänkäjärvi (Fig. 1), hereafter referred to as the OS lake, during summer 2017. The MS lake fluxes were measured on five days between June and October in 2017 and other five days between June and September 2018. The OS lake was measured biweekly during June – August 2017. The second year of the organic sediment (OS) lake were estimated by using the first year's measurements. The estimated second year OS lake fluxes were used for assessing the landscape level fluxes.

The flux measurements were conducted with floating flux chambers, while the CH_4 ebullition was determined from both chamber and floating bubble collector data. The diffusive fluxes of the MS lake were measured with an opaque aluminium chamber (60 cm × 60 cm × 30 cm) at 20 m from the north shore. The chamber air was mixed with a battery-driven fan. The closure time was 7 min, after which the chamber was ventilated for 3 min. The changes in CO_2, CH_4 and H_2O mixing ratios inside the chamber were measured using a closed-path infrared gas analyser (Picarro G2401, Picarro Inc, USA) connected to the chamber via a 50 m long inlet tube (Teflon, inside diameter 3.1 mm). On the OS lake, floating chambers with a volume of 8 L and an area of 0.05 m^2 were applied, using a 30-60 min closure. Four samples (30 mL) of gas space were drawn using polyethene syringes, and the samples were stored in 12 mL glass vials flushed with sample air. Samples were analysed within

https://doi.org/10.5194/bg-2022-69
Preprint. Discussion started: 6 April 2022

a month using a gas chromatograph equipped with EC, TC and FI detectors (Agilent 7890B, with Gilson GX271 autosampler). We tested CO_2 concentrations and fluxes against those measured using an on-line CO_2 sensor (K33 ELG CO_2 module, Senseair) in one of the chambers, and obtained similar flux values. In all, five to ten chambers were deployed at the time. The chambers were lined with a rope, anchored in both ends, so that they captured a water segment extending from about 20 m from near shore towards the lake centre. The chambers captured some ebullition events, and these were accounted as bubble flux. In addition, funnel bubble collectors with an area of 0.03 m^2 were floated. The auxiliary flux measurements from three lakes outside the study area was conducted with the same method as for OS lake. These measurements were utilised to assess the representativeness of the flux data collected on the MS and OS lakes.

The CO_2 and CH_4 diffusive fluxes were calculated from the change in CO_2 and CH_4 mixing ratios inside the closed chamber. The rate of change was calculated with linear regression based on ordinary least squares, similarly to the fen ecosystem chamber measurements by Heiskanen et al. (2021).

The measurement data of diffusive fluxes were screened to reject cases with non-linear concentration change and disturbances due to chamber leakage and ebullition events. The number of accepted/total data of the MS lake fluxes was 54/56 in 2017 and 62/75 in 2018. The number of accepted/total data of the OS lake diffusive CO_2 fluxes was 42/50 and diffusive CH_4 fluxes 49/50. There were ebullition events in 7 % of the individual flux measurements on the OS lake in 2017. This ebullition frequency was used to estimate the total ebullition-induced flux over the ice-free period.

2.3 Abiotic and biotic environmental measurements

In addition to the C flux measurements, meteorological and environmental variables were measured continuously at and close to the flux measurement locations in the pine forest, fen and lake ecosystems. Air temperature, precipitation sum and snow depth were measured at the weather station of the Finnish Meteorological Institute, located between the pine forest and fen EC measurement sites. Air temperature and humidity (Vaisala HMP 230), global and reflected radiation (Kipp&Zonen CM7), and downward and upward PPFD (Kipp&Zonen PQS 1) were measured at the forest and fen sites at heights of 14 m and 3 m, respectively. Water vapour pressure deficit (VPD) was calculated from air temperature and relative humidity according to Jones (2013). Forest soil temperature (T_s) was measured at 5 and 10 cm depths (Onset, HOBO) and soil moisture at 10 cm depth (Onset, HOBO). T_s profiles at the fen were measured from a string (at 10, 30, 50, 75 and 105 cm depth) and flark (at 10, 30 and 50 cm depth) (IKES Pt100 sensors). The water table level (WTL) was measured manually from the flux chamber positions at the fen and OS lake, while the WTL of the MS lake was measured with a pressure sensor (Onset, HOBO U20) at the floating flux chamber position. Lake water temperature (Onset, HOBO Pedant) was measured at the same position at 10 cm from the lake bottom.

The ice-free period of the flux measurement lakes was determined from air temperature data and repeat digital photographs at the fen site. In October 2018, the lake freezing was recorded with a temperature and pressure logger (Onset, HOBO). The freezing occurred after air temperature remained continuously below 0 °C for three days with no subsequent exceedances. The timing of thaw was determined from the snowmelt and ice thaw at the fen.

https://doi.org/10.5194/bg-2022-69
Preprint. Discussion started: 6 April 2022

We defined meteorological drought on the basis of the atmospheric VPD as the period during which the daily maximum VPD (VPD_{max}) exceeded 20 hPa (Lindroth et al., 2007; Aurela et al., 2007).

The Standardised Precipitation Evapotranspiration Index (SPEI), which takes into account both precipitation and potential evapotranspiration in determining drought conditions (Vicente-Serrano et al., 2010), was used as a climatological reference for the study period. Monthly SPEI data covering the years 1950–2018 for the 0.5° × 0.5° grid cell including Kaamanen were extracted from the global SPEI database (SPEIbase v2.6, https://spei.csic.es/database.html, last access 19 October 2021).

2.4 Estimating pine bog flux

In the subarctic aapa mires, pine bogs typically form narrow zones bordering forests and peatlands. Conducting direct EC flux measurements on them is challenging, as the fetch is too limited for the EC method. Thus, the fluxes of the two pine bog ecosystems within the study area were not directly measured but, to enable regional upscaling, were modelled based on the fluxes measured in the forest and fen ecosystems. The use of forest and fen fluxes was considered appropriate, as the tree species composition in pine forest and pine bog is similar and the peat soil ground layer vegetation of pine bog is similar to that of the string top PCT at the fen (Table A1).

For estimating the pine bog fluxes, the total forest flux was assumed to consist of the flux of trees and the flux of the other forest ecosystem elements,

$$F_{\text{forest}} = F_{\text{forest,trees}} + F_{\text{forest,other}} \tag{2}$$

and similarly for the pine bog ecosystem:

$$F_{\text{pine bog}} = F_{\text{pine bog,trees}} + F_{\text{pine bog,other}}. \tag{3}$$

The ‘trees’ fluxes were assumed to be proportional to tree biomass, i.e.

$$F_{\text{pine bog,trees}} = \mathrm{a} \times F_{\text{forest,trees}}, \tag{4}$$

where a is the tree biomass ratio between pine bog and pine forest (a = 0.52 and 0.16 for treed and sparsely treed pine bog, respectively; Table A4; see Supplement for biomass measurements and maps). Assuming further that the ground layer (‘other’) fluxes in both forest and pine bog equal the flux of the fen’s driest PCT, i.e. string top,

$$F_{\text{forest,other}} = F_{\text{pine bog,other}} = F_{\text{string top}}, \tag{5}$$

Eqs. (2)–(5) show that the GPP and ER fluxes for the pine bog can be estimated as

$$F_{\text{pine bog}} = \mathrm{a} \times F_{\text{forest}} + (1 - \mathrm{a}) \times F_{\text{string top}}, \tag{6}$$

where F_{forest} and $F_{\text{string top}}$ are obtained from measurements.

2.5 Upscaling fluxes to landscape-level

The CO_2 and CH_4 fluxes of different ecosystems were upscaled to landscape-level by taking into account the areal contributions inside the 7 km^2 study area (Table 1) and summing the half-hourly area-weighted NEE, GPP, ER and CH_4 flux estimates of each ecosystem. The pine forest and pine bog daily average growing season CH_4 flux estimates were taken from literature

https://doi.org/10.5194/bg-2022-69
Preprint. Discussion started: 6 April 2022

(Bubier et al., 2005; Dinsmore et al., 2017), which were further calculated for 180 day long growing seasons at Kaamanen. The annual balances of the OS lake were estimated for the second study year from the previous year's measurements by scaling with the ice-free period length.

2.6 Estimating flux uncertainty

The uncertainty of the EC-based CO_2 and CH_4 flux sums of the pine forest and fen ecosystems were estimated by taking into account the most significant error sources similarly to the method described in Heiskanen et al. (2021). The random error was estimated for the statistical measurement error and the error caused by gap-filling of missing data (Räsänen et al., 2017). Additionally, the annual error due to friction velocity filtering was estimated by recalculating the annual EC-based CO_2 and CH_4 balances with modified data sets that were screened with two additional friction velocity limits (pine forest: 0.19 and 0.31 m s^{-1}, fen: 0.05 and 0.15 m s^{-1}). This error was calculated as the average deviation from the annual balance calculated with the optimal friction velocity limit (pine forest: 0.24 m s^{-1}, fen: 0.1 m s^{-1}) (Aurela et al., 2002).

For the flux chamber-based monthly CO_2 and CH_4 flux sums of the lake ecosystem, the measurement uncertainty was estimated from the standard deviation of the flux data from the repeated chamber closures. The uncertainty of the annual CO_2, CH_4 and C flux sums were accumulated as the root sum square of individual uncertainties.

For the modelled pine bog fluxes, both for treed and sparsely treed bogs, the uncertainty was combined from the pine forest string top flux uncertainties proportionally to their contribution to the derived flux. The string top flux uncertainty was estimated by combining the uncertainty due to the estimated parameters of environmental response functions and the flux variation among the chamber plots (Heiskanen et al., 2021).

The landscape-level flux uncertainty was calculated by combining the total uncertainties of each ecosystem proportionally to their areal coverages (Table 1).

2.7 Statistical analysis

The estimates of monthly ER, GPP, NEE and CH_4 exchange of each ecosystem were compared between the two growing seasons using Welch's t test for the lake data, which comprised a sample of measured fluxes, and the Z test for the other ecosystems, for which we produced full flux time series with uncertainty estimates.

For identifying the main environmental drivers of the pine forest CO_2 flux, a linear regression model was estimated to explain the 5-day averaged GPP and ER fluxes derived from the EC data. The F_R data were normalised to 10 °C (denoted as F_{R10}), while the F_{GPP} data were normalised to a near-optimal PPFD level of 1200 µmol m^{-2} s^{-1} (denoted as $F_{GPP1200}$) (Laurila et al., 2001).

The following fixed explanatory 5-day variables were tested in the models: precipitation sum, average VPD_{max}, soil moisture and temperature at a depth of 10 cm, air temperature and daily maximum PPFD. T_s was included in the final analysis while air temperature was excluded, because these variables were strongly correlated (Pearson's R = 0.96 in the F_R data and R = 0.93 in the $F_{GPP1200}$ data) and T_s showed higher absolute correlation with the response variables. The MODIS Normalised Difference

https://doi.org/10.5194/bg-2022-69
Preprint. Discussion started: 6 April 2022

Vegetation Index was also tested as an explanatory variable, but it was excluded from the final analysis, as it strongly correlated with T_s (Pearson's R = 0.87 in the F_R data and R = 0.89 in the $F_{GPP1200}$ data). For the final models, the explanatory variables were chosen with a stepwise procedure to both directions by minimising Akaike's information criterion value. To evaluate the relative impact of each explanatory variable, the standardised regression coefficients were calculated. Data analyses were conducted in R (R Core Team, 2021) with the packages MASS (Venables and Ripley, 2002) and MuMIN (Barton, 2020).

3 Results and discussion

3.1 Environmental conditions

We studied CO_2 and CH_4 fluxes across different ecosystem types in Kaamanen from June 2017 to June 2019. The growing seasons (May–October) of 2017 and 2018 differed from each other in terms of their meteorological conditions, which affected the CO_2 and CH_4 exchange between the atmosphere and ecosystems. The early growing season in 2017 was colder than the corresponding period in 1981–2010 on average (Pirinen et al., 2012), with May being 1.9 °C and June 1.4 °C colder (Fig. 3). The summer months June–August were rainy in 2017, which was reflected in cloudiness that decreased the incoming solar radiation, with July in particular being cloudy (Fig. 4). In contrast, the spring of 2018 was warm, with May being 3.8 °C warmer than the 30-yr May average. In July 2018, a widespread drought and heatwave event in north-west Europe reached Kaamanen and caused the monthly mean air temperature to rise to 18.6 °C, which was 5.3 °C higher than the 30-yr July average. Additionally, the monthly precipitation sum was less than half of the 30-yr average (34 and 72 mm, respectively). After the drought, the following August and September were also warmer than the corresponding 30-yr averages, by 1.5 and 1.9 °C, respectively, but precipitation sum was then double the 30-yr average. The spring 2019 was characterised by a dry and warm April (3.7 °C above the long-term average) and rainy weather in May and June. Lake water levels were visibly lower in 2018 exposing the shoreline sediments of shallow lakes, for instance in the MS lake of this study.

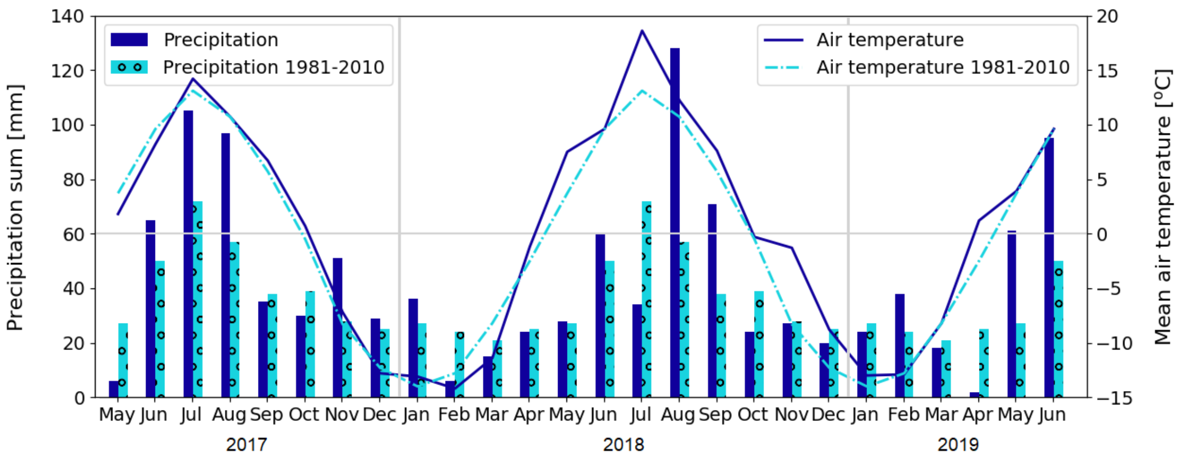

Figure 3. Monthly precipitation sum and mean air temperature at Kaamanen, and the corresponding 30-yr averages (Pirinen et al., 2012) measured at the Ivalo weather station (68°36' N, 27°25' E; 59 km south of Kaamanen).

https://doi.org/10.5194/bg-2022-69
Preprint. Discussion started: 6 April 2022

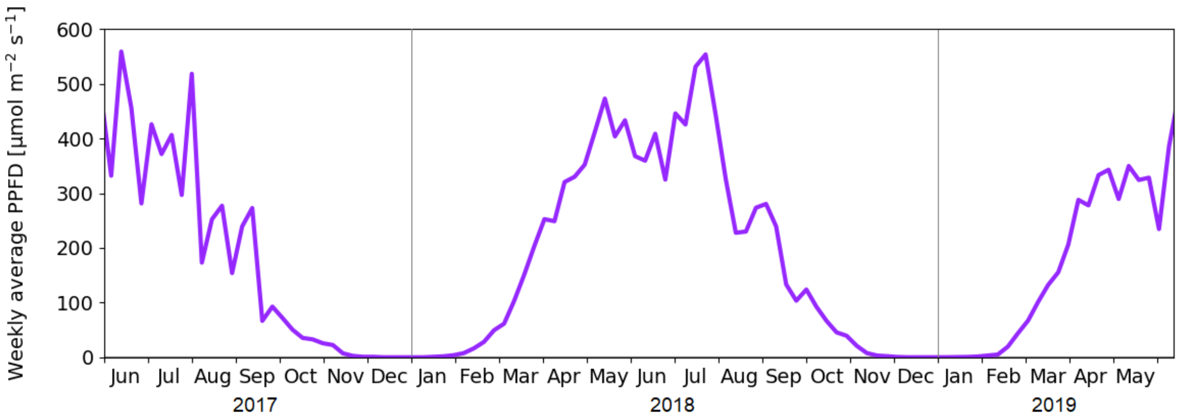

355 **Figure 4.** Weekly average photosynthetic photon flux density (PPFD) measured at Kaamanen.

The forest soil freeze and thaw occurred each year in the end of October and mid-May, respectively (Fig. 5a). In late autumn 2018, the forest T_s decreased from 8 °C to 1 °C in just 20 days between 23 September and 13 October, which was due to the lack of snow cover. In the fen, the surface peat of the strings froze concurrently with the forest soil (Fig. 5b). However, the thaw occurred slightly earlier in the strings than in the forest, where trees shaded the surface. The continuous water saturation in the flark peat led to weaker peat temperature responses to changing air temperature than in the dryer strings. The lake water temperature, measured only during the ice-free periods of 2017 and 2018 (Fig. 5c), was affected, in addition to air temperature, by the incoming flow to the lake and by the water level. Following the air temperatures, the forest soil, fen peat and lake water temperatures were higher in July 2018 than in 2017.

https://doi.org/10.5194/bg-2022-69
Preprint. Discussion started: 6 April 2022

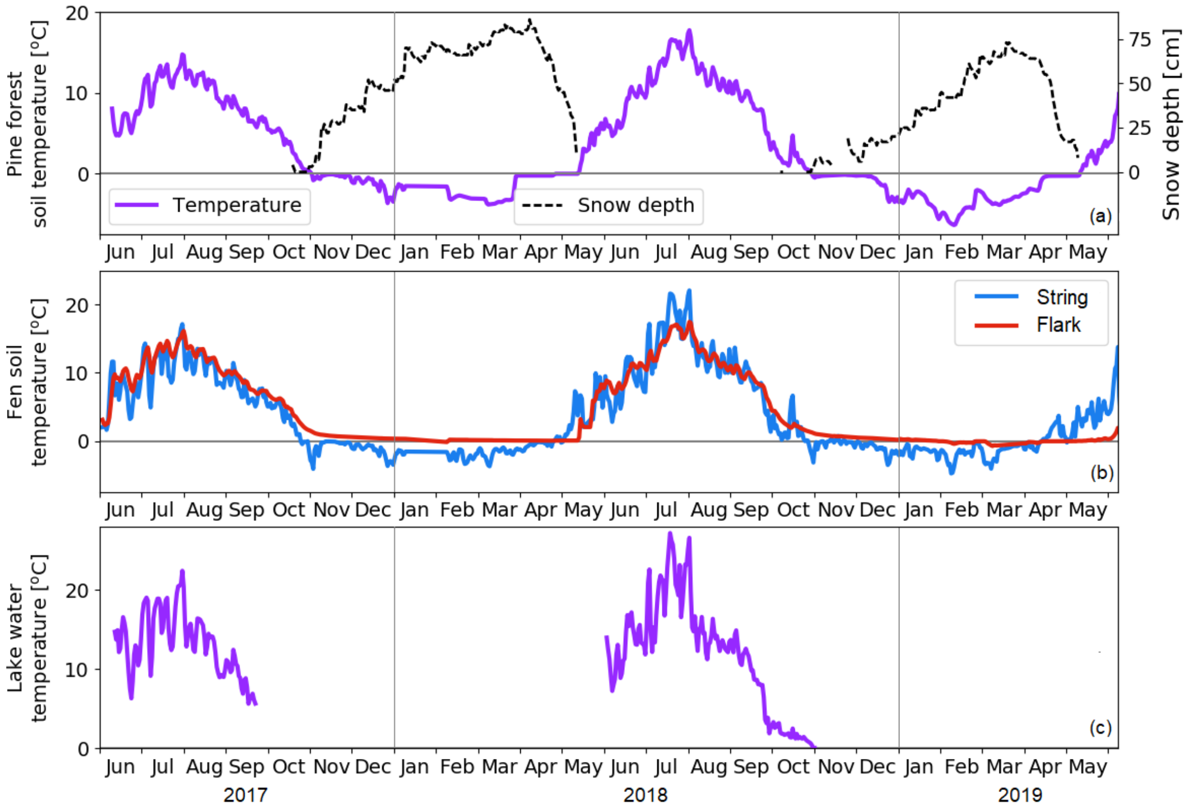

Figure 5. Daily average (a) forest soil temperature measured at 10 cm depth and snow depth, (b) fen peat temperature measured from strings and flarks at 10 cm depth and (c) MS lake water temperature at of the floating chamber position 10 cm from the bottom.

The ice-free period of the measured lakes lasted for 167 and 176 days (from May to October) during the first and second study year, respectively (Table 4).

Table 4. Estimated ice-free period start and end dates of the studied lakes.

Period start	Period end
25 May 2017	26 October 2017
10 May 2018	30 October 2018
5 May 2019	19 October 2019

The meteorological drought lasted from 2 July to 1 August 2018 (Fig. 6a). The drought limit of daily VPD_{max} 20 hPa was exceeded on 13 days in total in 2018, while no exceedances took place in 2017. The average daily maximum VPD in 2 July – 1 August 2018 was 16.9 hPa, while during the same period in 2017 it was 9.4 hPa. The corresponding daily air temperatures were 18.5 and 14.2 °C, respectively. The highest daily maximum VPD of 31 hPa was observed on 18 July 2018. VPD responded rapidly to the reduced amount of water in the environment, while the water table level in the fen, the water depth of lakes and the forest soil moisture decreased gradually as the drought developed (Fig. 6).

https://doi.org/10.5194/bg-2022-69
Preprint. Discussion started: 6 April 2022

Within the fen, WTL varied strongly among the plant community types (Fig. 6b). In the flark and *Trichophorum* tussock PCTs, WTL was most of the time close to or at the peat surface, while in elevated strings it was deeper from the peat surface, fluctuating between -10 and -20 cm in string margins and between -30 and -70 cm in string tops. The drought decreased the WTL in all plant communities simultaneously, and by mid-August WTL had recovered to a normal level except for the string tops.

The water depth of the MS lake was within 30–40 cm (Fig. 6c) and it dropped in June–July 2018 to less than 20 cm in the centre of the lake. This drawdown was associated with a shoreline retreat of 6 to 8 m. However, after the first rainfall in 3–5 August, the water depth quickly reverted to the pre-drought level. Our field observations and visual interpretation of satellite and drone imagery suggest that the water level drop magnitude was uniform in the waterbodies within the study area.

The annual cycle of the soil moisture measured in the pine forest showed a low moisture content (< 0.1 $m^3\,m^{-3}$) during winter and fluctuations after the soil thaw (Fig. 6d). During both springs, the water availability in soil was at its maximum in 10–14 May due to melting snow. The drought during summer 2018 was clearly indicated by the soil moisture data that showed a drastic drop from 0.2 to 0.1 $m^3\,m^{-3}$ between 23 June and 22 July. After the rainfall in the beginning of August, soil moisture rose in a few weeks to the average growing season level. Thus, even though the meteorological drought was already over in the beginning of August, the water availability to vegetation was not yet fully recovered.

In terms of the drought index (SPEI), the drought event in July 2018 was the eighth most severe drought in Kaamanen between January 1950 and December 2018 (Fig. 7). However, the drought event was relatively short, and the five-month SPEI between May and September was close to neutral.

https://doi.org/10.5194/bg-2022-69
Preprint. Discussion started: 6 April 2022

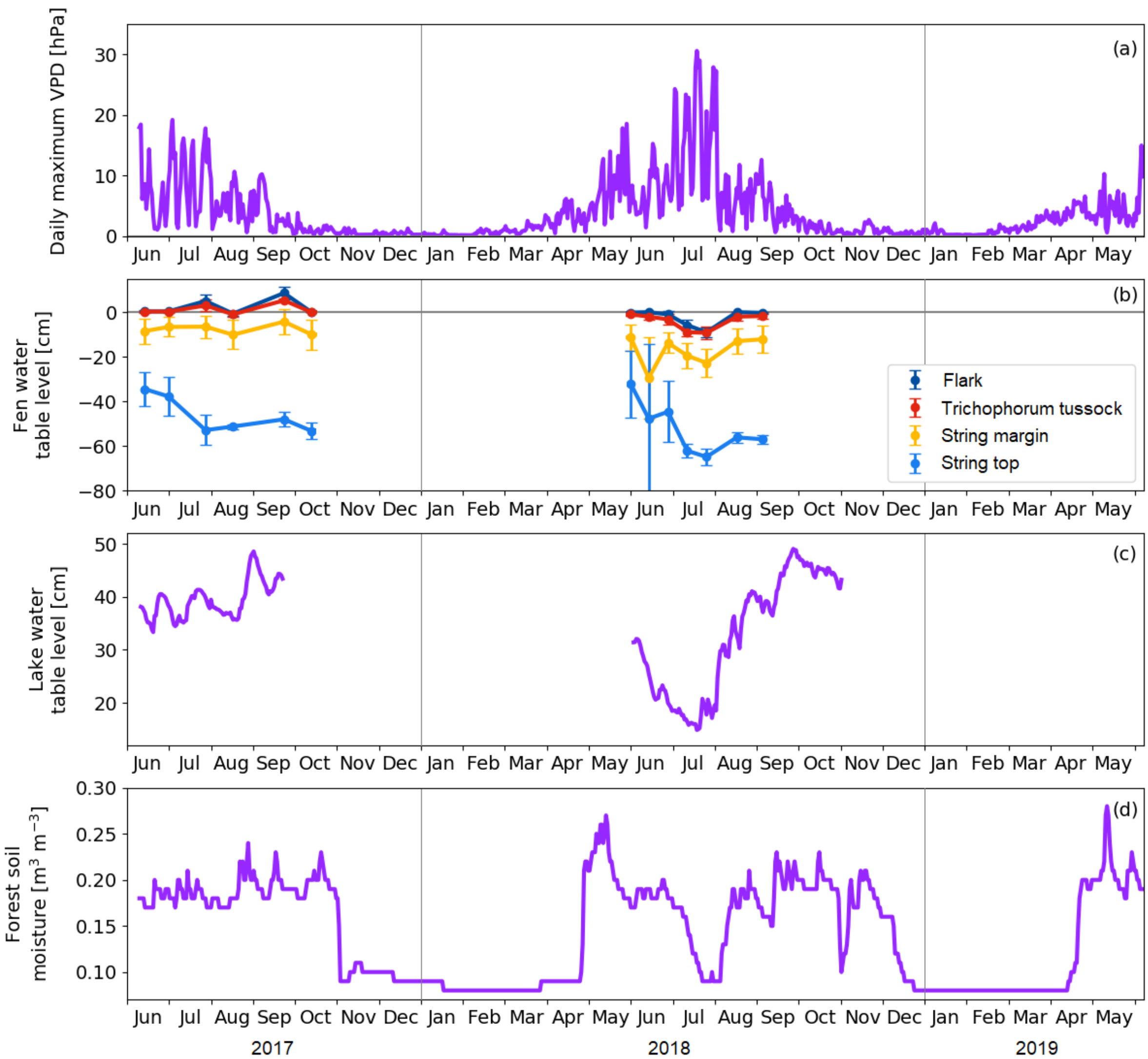

395

Figure 6. (a) Daily maximum vapour pressure deficit. (b) Mean water table level at the main plant communities of the fen. Error bars represent the standard deviation. (c) Water table level at the floating chamber position in Lake Jänkälampi. (d) Forest soil moisture at 10 cm depth.

https://doi.org/10.5194/bg-2022-69
Preprint. Discussion started: 6 April 2022

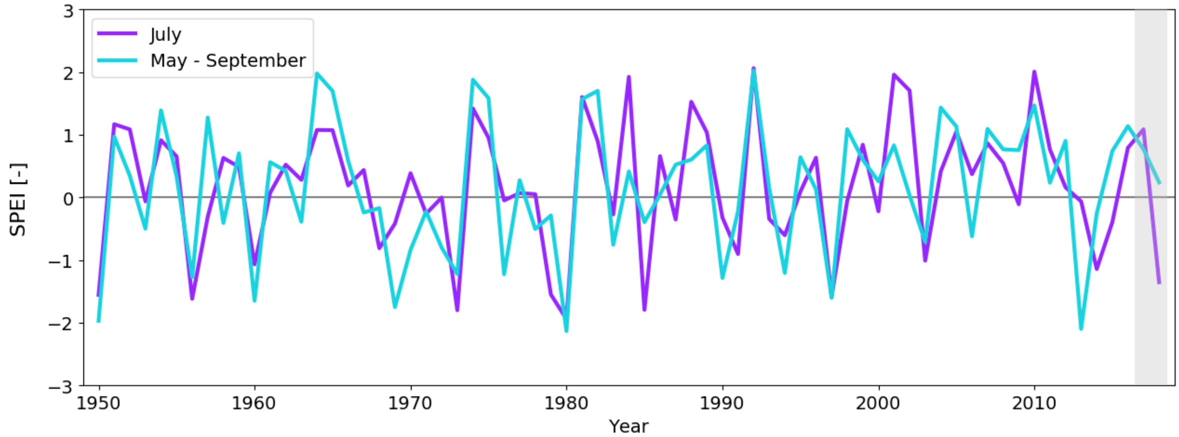

Figure 7. One month (July) and five-month (May-September) Standardised Precipitation Evapotranspiration Index (SPEI) time series at Kaamanen 1950 – 2018. Positive SPEI values denote moist conditions and negative values drought conditions. Years 2017 and 2018 are marked with shading.

3.2 Ecosystem CO_2 and CH_4 fluxes

3.2.1 Pine forest fluxes

The pine forest acted as a net CO_2 sink during both study years. The annual CO_2 balances during the first and second study year were -78.3 ± 50.8 and -118.9 ± 26.8 g C m^{-2}, respectively (Fig. 8b, Table A5). Notably, the Kaamanen site is located about 150 km north to the other studied evergreen needleleaf forests in the region. Observations have shown that such forests in northern Fennoscandia region have acted as small annual CO_2 sinks (Aurela et al., 2015). The growing season (11 June – 31 October) GPP and ER sums were larger during the first measurement year than the second one (Table A6).

There were three distinct periods during which the CO_2 fluxes diverged between the years, resulting in the difference in the annual balance. The first dissimilarity was that ER rates were larger during 15 June – 15 August 2017 compared to the same period in 2018 (Figs. 8c, A1). This was caused by the higher-than-average precipitation sum in 2017 (Fig. 3), which saturated or nearly saturated the soil with water throughout the peak growing season. As the forest soil moisture was continuously close to the maximum water holding capacity, the effect of abundant precipitation emerged as increasing lake water table levels (Fig. 6c-d). We suspect that the higher ER in 2017 was caused by enhanced heterotrophic soil respiration, which is known to increase with soil moisture until near water saturation (Orchard and Cook, 1983; Moyano et al., 2012; McElligott et al., 2017; Du et al., 2020).

The second period of dissimilar CO_2 fluxes was observed when the drought and heatwave discussed above limited fluxes in 2018. Compared to the previous year, GPP was reduced in 22 July–17 August and ER in 26 July–15 August 2018 (Fig. 8c-d). The daily maximum VPD surpassed the 20 hPa limit, indicating meteorological drought, for the first time on 2 July and the last time on 1 August 2018 (Fig. 6a), during which period the average air temperature was 5 °C higher than in the previous year (Fig. 3). In July 2018, the forest soil moisture at 10 cm depth also dropped by 50 % from the normal growing season level, reaching 0.1 m^3 m^{-3} on 22 July (Fig. 6d). Soil moisture recovered to a normal level three weeks later on 13 August.

There is evident discrepancy between the timing of meteorological drought and reduced ecosystem CO_2 fluxes. The response to drought in plants occurs both in roots, where water availability through soil is a key factor, and in the stomatal openings in leaves, where the gas exchange is affected by stomatal control due to VPD. The tighter stomatal control due to high VPD limits C assimilation (Martín-Gómez et al., 2017), and in Scots pine trees this has been estimated to occur at a VPD of 8 hPa while at approximately 28 hPa the stomata are fully closed (Büker et al., 2012). The drought seemed to have an effect on the CO_2 exchange until 18 August, even though soil moisture and VPD hardly had any direct effect anymore, as only after this date the magnitude of ER and GPP fluxes were not continuously lower compared to the previous year. This lagged effect could be caused by embolism, defoliation or root degradation (Aguadé et al., 2015), or by weakened mycorrhizal symbiosis in the roots (Muilu-Mäkelä et al., 2015). Gao et al. (2017) also found that the GPP of a southern boreal Scots pine forest was suppressed during a severe soil moisture drought in the summer of 2006 as the plants regulated their stomata due to high VPD.

The third period of dissimilarity was observed in autumn between 25 September and 12 October and in a smaller scale within 17–30 October, when the ER fluxes were lower in 2018 than 2017. This was due to the soil temperature decrease from 8 ºC to 1 ºC between 23 September and 12 October and again from 5 ºC to 0 ºC within 15–30 October. Due to the drop in ER fluxes in 2018, the forest ecosystem momentarily turned into a CO_2 sink.

According to the linear regression model, the main environmental factors affecting the radiation-normalised GPP flux ($F_{GPP1200}$) of the pine forest were T_s, VPD_{max} and soil moisture (Table 5). The magnitude of $F_{GPP1200}$ increased with increasing T_s and soil moisture and decreased with increasing VPD_{max}. The positive correlation with soil moisture originated from the anomalously low moisture levels during the 2018 drought (Fig. 6d). The temperature-normalised respiration (F_{R10}) was affected by T_s, VPD_{max}, soil moisture and precipitation sum (Table 5). F_{R10} increased with increasing T_s, soil moisture and precipitation sum, and decreased with increasing VPD_{max}.

https://doi.org/10.5194/bg-2022-69
Preprint. Discussion started: 6 April 2022

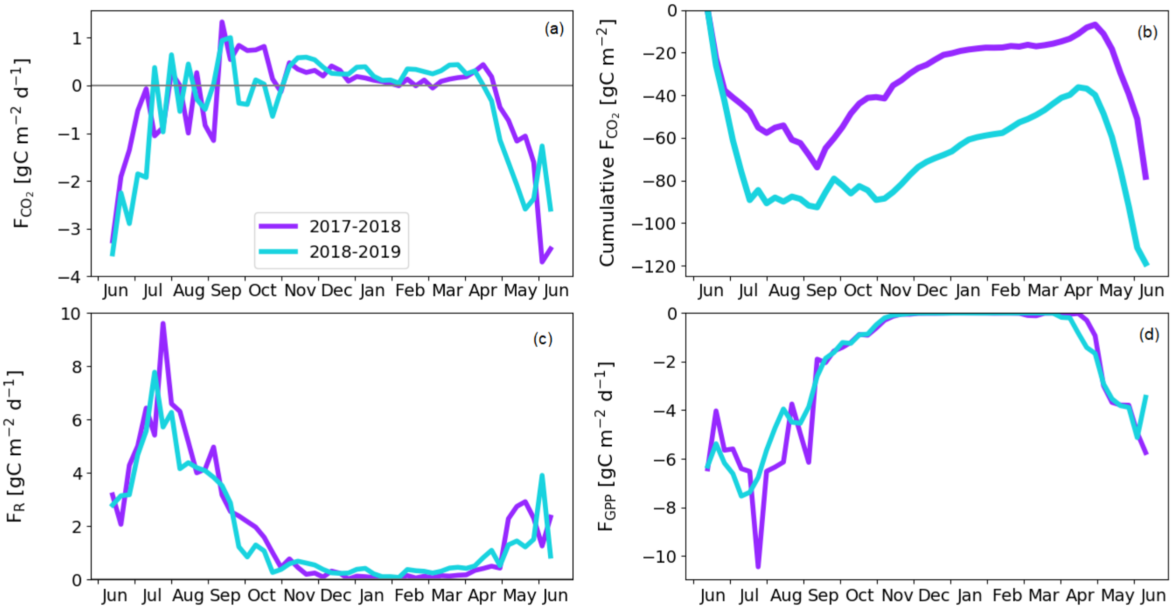

445 **Figure 8.** Pine forest fluxes. Weekly averaged (a) and cumulative (b) CO_2 flux, and weekly averaged ecosystem respiration (c) and gross primary productivity (d).

Table 5: Standardised regression coefficients (± standard error) for the explanatory variables of the linear regression model for EC-based $F_{GPP1200}$ and F_{R10}. The adjusted coefficient of determination (R_a^2), normalised root mean square error (nRMSE; RMSE divided by the range
450 of response variable values) and degrees of freedom (df) are also shown.

	Regression coefficient	df
$F_{GPP1200}$ (R_a^2 = 0.78, nRMSE = 0.12)		
T_s (-10cm)	-1.02 ± 0.11	34
VPD_{max}	0.28 ± 0.11	34
Soil moisture (-10cm)	-0.17 ± 0.08	34
F_{R10} (R_a^2 = 0.68, nRMSE = 0.15)		
T_s (-10cm)	0.87 ± 0.18	31
VPD_{max}	-0.78 ± 0.18	31
Soil moisture (-10cm)	0.24 ± 0.12	31
Precipitation sum	0.21 ± 0.11	31

https://doi.org/10.5194/bg-2022-69
Preprint. Discussion started: 6 April 2022

Biogeosciences Discussions
Open Access

3.2.2 Fen fluxes

The fen ecosystem was a net CO_2 sink during both study years. The annual CO_2 balance was -20.6 ± 3.6 and -7.6 ± 3.7 g C m^{-2} during the first and second year, respectively (Fig. 9b, Table A5). There were two periods during which the CO_2 fluxes diverged between the years: the start of the growing season and a drought and heatwave event in 2018.

The earlier start of the growing season in 2018 resulted in a higher CO_2 uptake in 11–30 June compared to the previous year (Fig. 9, Table A6); the balances were -4.8 ± 6.4 and -21.0 ± 10.1 g C m^{-2} in 2017 and 2018, respectively. This was due to the nearly doubled GPP, which was 27.6 ± 3.9 and 49.2 ± 7.3 g C m^{-2} in 2017 and 2018, respectively. The increase of net CO_2 uptake in northern mires due to earlier snowmelt and warm spring temperatures has been reported previously by e.g. Aurela et al. (2004) and Sagerfors et al. (2008). The differences in CO_2 exchange between the microforms of the fen were studied in more detail by Heiskanen et al. (2021), who found that the magnitude of ER and GPP increased gradually from the wettest PCT, i.e., flark, to the driest one, i.e., string top. However, the variation in net CO_2 uptake among the microforms was weaker than in the two flux components. The increased GPP due to warm spring weather was observed in all main microforms. However, the simultaneous increase in ER led to a significantly ($p < 0.05$) higher net CO_2 uptake only in string tops, when comparing the early growing seasons of 2017 and 2018 (Fig. A2).

The higher CO_2 uptake during the early growing season of 2018 was offset by the decreased uptake due to the drought and heatwave event in 20 July – 9 August 2018. As discussed above, the drought was observed as higher-than-average temperatures (Fig. 3), an elevated VPD (Fig. 6a) and water level drawdown by 5–20 cm at the fen microforms (Fig. 6b). These anomalies likely caused drought stress in the mire plants (Alm et al., 1999). The drought stress reduced GPP and the high temperatures increased ER compared to the previous weeks and the same time period during the previous year (Fig. 9c,d). The CO_2 uptake decreased during this period, and at the end of the period the fen ecosystem even turned into a CO_2 source. Unlike the increased CO_2 uptake during the early growing season, which could be allocated largely to the string plant communities, the drought affected plant communities in all microforms (Heiskanen et al., 2021). The CO_2 exchange in flarks including *Trichophorum* tussocks was immediately affected by the lowering WTL in July and August 2018 (Fig. 6b), while the drier string communities were affected to a lesser extent.

While the fen was an annual net CO_2 sink it also acted as a CH_4 source to the atmosphere during both study years. The annual CH_4 balance was 7.0 ± 0.2 and 6.3 ± 0.3 g C m^{-2} during the first and second study year, respectively (Fig. 9f). The flark, *Trichophorum* tussock and string margin PCTs contributed 98 % of the emissions, with string margins accounting for 44 % of the emissions during the growing season of 2017 and all three having similar emissions in 2018 (Heiskanen et al., 2021).

The drought decreased the annual CH_4 emissions, mostly during 21 July – 28 August 2018, when the emissions were 0.8 g C m^{-2} lower than during the same period in the previous year (Fig. 9e). Notably, the decrease in CH_4 emissions occurred a few weeks after the meteorological drought begun and continued well after the WTL had reverted to the pre-drought level. The decrease in CH_4 emissions is likely due to both reduced release of carbon compounds by plant roots and increased oxic soil zone, which reduced CH_4 production and increased CH_4 oxidation (Strack and Waddington, 2008; White et al., 2008; Deppe

https://doi.org/10.5194/bg-2022-69
Preprint. Discussion started: 6 April 2022

et al., 2010). The lagged recovery of CH_4 flux coinciding with the GPP recovery indicates the link between methanogenesis and plant root exudates. Unfortunately, the uncertainties of the monthly CH_4 balances derived from the manual chamber measurements were large and the lower emissions could not be allocated to any specific PCT. However, the CH_4 emissions from flarks were larger in 2018 than 2017, which suggests that the drought-induced decrease in emissions occurred on the *Trichophorum* tussock and string margin PCTs that had lower WTL (Fig. 6b) (Heiskanen et al., 2021). The drought, which covered large parts of north-western Europe, did not affect the CO_2 and CH_4 exchange at Kaamanen as much as it did at more southern mires, where the drought duration was longer, although the water level draw down was similar in magnitude (Rinne et al., 2020).

The total carbon balance, i.e. the sum of the CO_2 and CH_4 fluxes, showed that the fen was an annual carbon sink of -13.6 ± 3.6 g C m^{-2} and carbon neutral, -1.3 ± 3.7 g C m^{-2}, in the first and second study year, respectively (Table A5). The lower CO_2 uptake during the drought period contributed most of the difference between the years. Previous studies at the Kaamanen fen show that the ecosystem has been on average a larger annual CO_2 sink: −22 g C m^{-2} (from -4 to -53 g C m^{-2}) during 1997–2002 (Aurela et al., 2004), and similar average annual CH_4 source: 6 g C m^{-2} for 1995, 1997–1998 and 2011–2016 (Hargreaves et al. 2001; Piilo et al., 2020).

https://doi.org/10.5194/bg-2022-69
Preprint. Discussion started: 6 April 2022

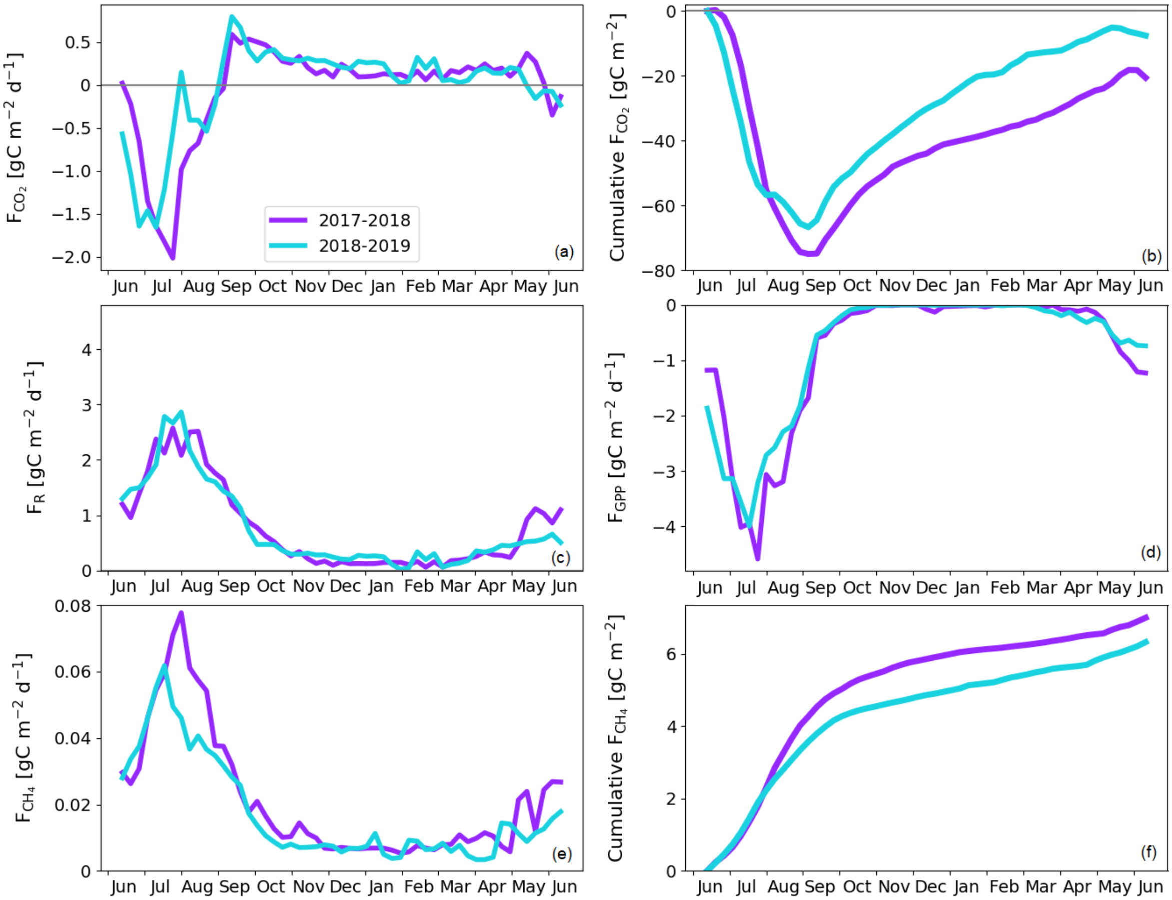

Figure 9. Fen fluxes. Weekly averaged CO_2 (a), ER (c), GPP (d) and CH_4 (e) flux, and cumulative CO_2 (b) and CH_4 (f) flux.

3.2.3 Lake fluxes

The annual CO_2 and CH_4 balances of the study lakes were estimated from the fluxes measured during the ice-free period assuming no flux in winter. During the first study year starting on 11 June 2017, the lakes were free of ice in 11 June – 26 October 2017 and 10 May – 10 June 2018 and during the second year in 11 June – 30 October 2018 and 5 May – 10 June 2019 (Table 4). The C fluxes were measured during both years only on the mineral sediment (MS) lake, while the second-year balances of the organic sediment (OS) lake, needed for landscape-level upscaling, were estimated from the first year's measurements. The estimated CO_2 emissions were 11.1 ± 3.5 and 14.2 ± 2.0 g C m^{-2} from the MS lake during the first and second ice-free period, respectively, and 74.7 ± 28.4 g C m^{-2} from the OS lake during the first year. This can be explained by the fact that the OS lake is situated immediately downstream from the fen (Fig. 1), and thus has a higher C content in the sediment (30.3 % C of dry mass) than in the MS lake (5.5 – 22.6 % C of dry mass, depending on location) (Table A7) and receiving the transported OC in the stream flow.

https://doi.org/10.5194/bg-2022-69
Preprint. Discussion started: 6 April 2022

Both lakes showed largest CO_2 emissions in early June, right after the thaw (Fig. 10a), which were likely associated with the turnover caused by the break-down of thermal stratification. At the MS lake, the flux measurements covered also the autumn turnover mixing in September, when CO_2 emissions increased compared to the previous month. While the CO_2 emissions were influenced by the turnover mixing, a similar effect was not observed for CH_4 on either of the lakes. The daily CO_2 emissions of the OS lake (0.2–0.8 g C m^{-2} d^{-1}) were similar in magnitude, for instance, to those (0.3–1.4 g C m^{-2} d^{-1}) observed for Lake Stortjärn in Krycklan, Sweden, which is a northern boreal lake and also adjacent to a mire (Denfeld et al., 2020). In a similar shallow subarctic lake next to a fen at Abisko, Jammet et al. (2017) found high CO_2 emissions of 33.3 g C m^{-2} during the spring period of 41 days, but photosynthesis during summer reduced the net emission of the ice-free period to 8.9 g C m^{-2}. Lohila et al. (2015) estimated an annual CO_2 balance of 33 g C m^{-2} for the shallow parts of the large subarctic Lake Pallasjärvi and recorded small CO_2 uptake during midday in the summer months. This shows that the CO_2 balance of lakes varies substantially from lake to lake in the subarctic region. In Kaamanen, we did not observe notable CO_2 uptake by either of the lakes studied.

The annual CH_4 emissions through diffusive flux were 0.4 ± 0.2 and 0.7 ± 0.2 g C m^{-2} from the MS lake during the first and second ice-free period, respectively, and 2.4 ± 0.2 g C m^{-2} from the OS lake during the first year. We estimated that the CH_4 emissions through ebullition were 0.7 ± 0.2 g C m^{-2} from the OS lake during the first year and 0.1 ± 0.1 and 0.2 ± 0.1 from the MS lake during the first and second ice-free period, respectively. On the MS lake the CH_4 emission were higher in September 2018 than 2017 (Fig. 10b), likely due to warmer sediments and lower WTL (Figs. 5c, 6c).

The average daily diffusive CH_4 fluxes in Kaamanen (OS lake 0.014 g C m^{-2} d^{-1}, MS lake 0.003 g C m^{-2} d^{-1}) were similar to those reported in previous studies of boreal lakes (Fig. 10). Denfeld et al. (2020) observed a range of 0.001–0.008 g C m^{-2} d^{-1} for Lake Stortjärn during the open-water period, while Rasilo et al. (2014) found spatially highly variable CH_4 diffusive fluxes of 0.008 ± 0.020 g C m^{-2} d^{-1} across 224 boreal lakes in Canada during summer.

Our estimate of ebullition was 21 % of the total CH_4 emission from the Kaamanen lakes. Ebullition has been estimated to contribute 40–80 % of the total CH_4 emissions from open subarctic lakes (Bastviken et al., 2004; Wik et al., 2013; Jansen et al., 2020). The magnitude of annual CH_4 emissions of these lakes was 1.0–8.3 g C m^{-2} (Bastviken et al., 2004; Thornton et al., 2015; Jammet et al., 2017, to which range the Kaamanen lakes fall (OS lake 3.1 g C m^{-2}, MS lake 0.5–0.8 g C m^{-2}).

The estimated ebullition percentage of total emissions of Kaamanen lakes is conservative when comparing to other studies of boreal lakes, considering that the lakes in the Kaamanen area are mostly shallow (< 2 m deep) and thus likely to show more frequent CH_4 ebullition than deep lakes (Bastviken et al., 2004). In general, there is high temporal and spatial variation in ebullition as there are seep and non-seep areas where CH_4 bubbles emerge at the lake bottom, which complicates the ebullition estimation (Walter et al., 2006). Wik et al. (2018) found that the spatial ebullition potential was affected by the coarse detritus, buried aquatic vegetation and redeposited peat rather than the amount of total organic carbon or CH_4 in the sediment. The OS lake in our study had five times as much C as the MS lake (Table A7) and a layer of redeposited peat, which led to sevenfold CH_4 emissions compared to the MS lake.

The water level of the lakes decreased by about 15 cm during June–July 2018 as a result of drought and recovered to a normal level, similar to in 2017, quickly after the first rainfall in August (Fig. 6c), which changes could have affected the C fluxes.

https://doi.org/10.5194/bg-2022-69
Preprint. Discussion started: 6 April 2022

545 The monthly CO_2 flux on the MS lake was lower in July 2018 than in 2017 (p = 0.01), but no significant changes were observed in the CH_4 fluxes during the drought period.

Both lake types emitted 96 % of the total C efflux as CO_2 (Table 6). For comparison, in an extensive study of Alaskan subarctic lakes, the non-yedoma lakes emitted about 85 % as CO_2 and 15 % as CH_4 (Sepulveda-Jauregui et al., 2015), and in the above-mentioned 224-lake study the CH_4 diffusive fluxes contributed 8 ± 23 % to the total lake C emissions (Rasilo et al., 2014). The 550 MS lake emissions (Table 6) were very similar to those from Lake Kipojärvi, a nearby small (9.6 ha) lake surrounded by an esker and a peatland, for which an annual balance of 15 g C m^{-2} has been determined (Juutinen et al., 2013).

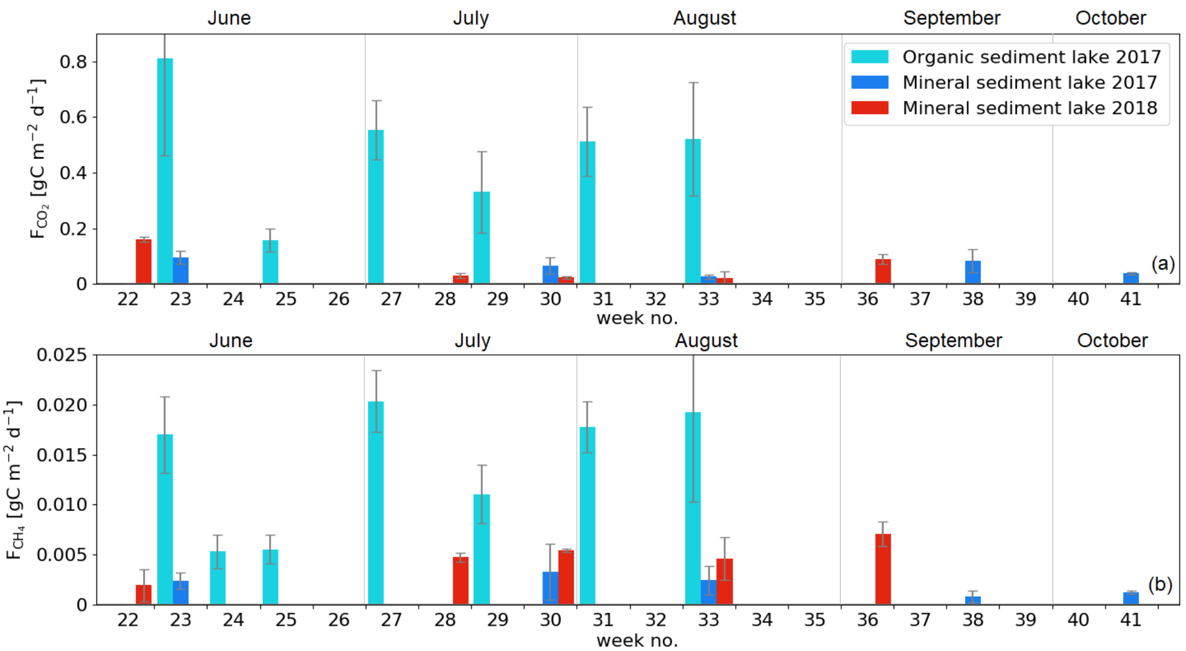

Figure 10. Weekly average lake CO_2 (a) and CH_4 (b) diffusive fluxes. Error bars represent the standard deviation of individual chamber measurements in each week.

555

Table 6. Estimated CO_2 and CH_4 fluxes [g C m^{-2}] of the MS and OS lakes and during the ice-free periods within the study years.

	11 June – 26 October 2017 & 10 May – 10 June 2018	11 June – 30 October 2018 & 5 May – 10 June 2019
Mineral sediment lake		
CO_2 flux	11.1 ± 3.5	14.2 ± 2.0
CH_4 diffusive flux	0.36 ± 0.20	0.65 ± 0.20
CH_4 ebullition flux	0.10 ± 0.06 [a]	0.18 ± 0.06 [a]
Total C flux	11.6 ± 3.5	15.0 ± 2.0
Organic sediment lake		
CO_2 flux	74.7 ± 28.4	

https://doi.org/10.5194/bg-2022-69
Preprint. Discussion started: 6 April 2022

CH_4 diffusive flux	2.44 ± 0.16
CH_4 ebullition flux	0.66 ± 0.16
Total C flux	77.8 ± 28.4

[a] Estimated from the ratio between CH_4 diffusive and ebullition fluxes of the organic sediment lake.

3.2.4 Pine bog fluxes

The treed pine bog ecosystem between the forest and fen ecosystems covers 9.1 % of the studied landscape, and the sparsely treed pine bog covers 13.5 % and is located within the fen ecosystem in the driest parts of peatland. The annual CO_2 balance of the treed pine bog ecosystem in the first and second study year was -39.1 ± 107.6 and -75.0 ± 111.2 g C m^{-2}, respectively (Fig. 11b, Table A5). While the annual CO_2 balance of sparsely treed pine bog ecosystem in the first and second study years was -9.8 ± 135.4 and -42.1 ± 145.3 g C m^{-2}, respectively (Fig. 12b, Table A5). The larger uncertainties of these balances compared to the forest and fen ecosystems were due to the contribution of the modelled string top fluxes, which were based on a limited number of chamber measurements (Sect. 2.4).

For both pine bog ecosystems, from mid-June to mid-July, the ER rates were slightly lower in 2018 than in 2017 (Figs. 11c, 12c), and at the same time the GPP rates were higher during the latter year (Figs. 11d, 12d). This led to larger net CO_2 uptake during the first part of growing season in 2018 than in 2017 (Figs. 11a,b, 12a,b, Table A6). However, this difference in fluxes was more prominent in the sparsely treed pine bog. The drought event decreased the magnitude of GPP rate similarly in both ecosystems between mid-July and mid-August 2018 to a lower level compared to the previous two summer months and the same period in 2017 (Figs. 11d, 12d, Table A6).

The pine bog ecosystem fluxes were derived from the pine forest and fen ecosystem fluxes. String tops, which were used as a proxy for a treeless pine bog, are relatively dry microsites with a typical water table depth of 40–60 cm (Fig. 6b). As part of the bog ecosystems are wetter than typical string tops, and as the flark PCTs at Kaamanen had lower CO_2 fluxes than the string tops (Heiskanen et al., 2021), the proxy approach may bias the pine bog flux estimates. However, the use of string margin fluxes instead of the string top fluxes would not make any significant difference. The fluxes of the pine bog ground layer have been studied previously within a nearby Kipojärvi catchment by Juutinen et al. (2013), who found that in 2006 the ground layer was an annual CO_2 sink of -130 ± 91 g C m^{-2}, with an annual GPP sum of -456 ± 77 g C m^{-2} and ER sum of 326 ± 48 g C m^{-2}. The ER sum was similar to that measured at the Kaamanen fen on the string top and margin PCTs (Heiskanen et al., 2021), but the magnitude of GPP sum was greater for the Kipojärvi catchment, which led to the annual CO_2 sink being smaller than for the Kipojärvi cathcment (Fig. A2b). This suggest that our pine bog flux model results might underestimate the ecosystem CO_2 sink.

https://doi.org/10.5194/bg-2022-69
Preprint. Discussion started: 6 April 2022

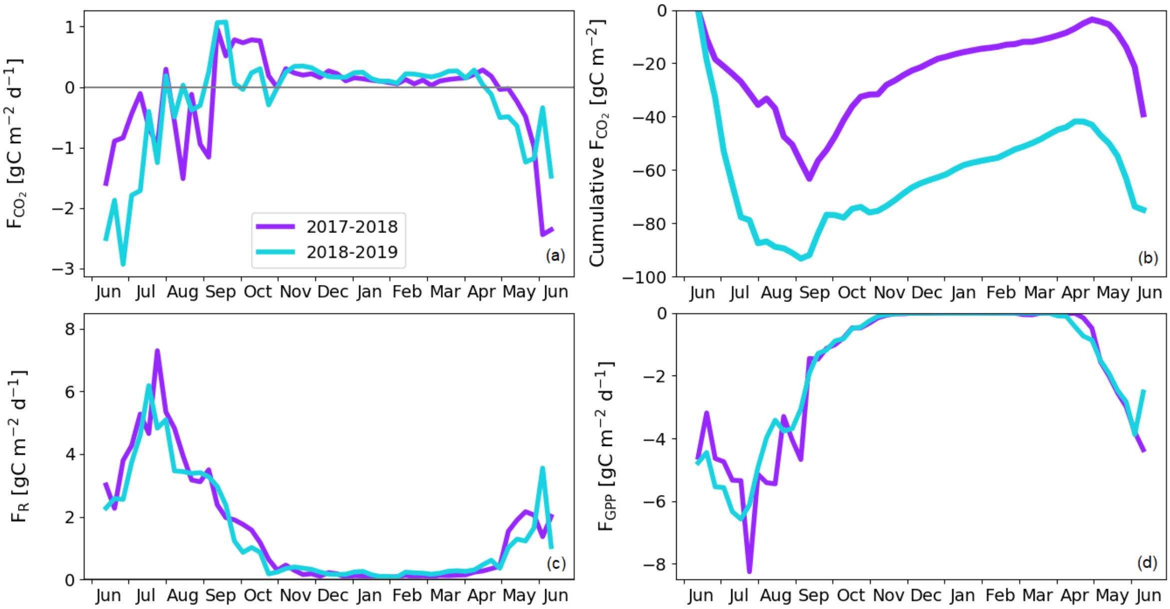

Figure 11. Treed pine bog fluxes. Weekly averaged CO_2 flux (a), and cumulative CO_2 flux (b), and weekly averaged ER (c) and GPP (d) flux.

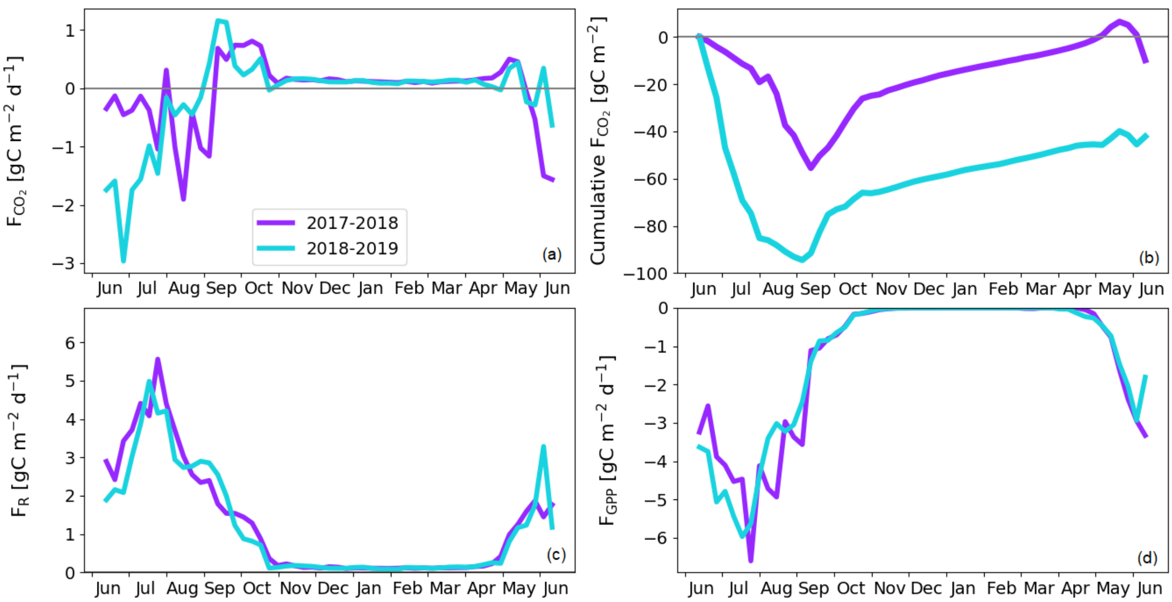

Figure 12. Sparsely treed pine bog fluxes. Weekly averaged CO_2 flux (a), and cumulative CO_2 flux (b), and weekly averaged ER (c) and GPP (d) flux.

https://doi.org/10.5194/bg-2022-69
Preprint. Discussion started: 6 April 2022

3.3 Upscaled landscape-level fluxes

By upscaling the ecosystem balances to our study area of 7 km^2, we obtained an annual landscape CO_2 balance of -25.9 ± 65.7 and -41.3 ± 64.9 g C m^{-2} for the two study years. The corresponding CH_4 balances were 2.4 ± 0.7 and 2.3 ± 0.7 g C m^{-2}, and the total C balances were -23.5 ± 65.7 and -39.0 ± 64.9 g C m^{-2}, respectively (Fig. 13 b,f, Table A5). The pine forest ecosystem contributed to the total landscape C balance with a large CO_2 sink and a minimal CH_4 sink. In the evergreen forest ecosystem, CO_2 uptake period was longer than that of the fen ecosystem: by 12 days in the beginning of the growing season and by 30 days at the end of the growing season (Figs. 8d, 9d), and during the first half of growing season the magnitude of CO_2 uptake was larger in the forest (Figs. 8a, 9a). The lake ecosystem was a complete opposite with substantial CO_2 and CH_4 emissions, while the fen ecosystem balances were between forest and lake with annual net CO_2 uptake and CH_4 emissions, although the fen had larger CH_4 emissions per unit area than the lake ecosystem. The pine bog ecosystems, which were modelled using pine forest and fen fluxes, most likely acted as CO_2 sinks and CH_4 sources. The magnitude of ecosystem-specific CH_4 emissions was much smaller than the magnitude of CO_2 exchange, with the exception of the fen ecosystem. The fen CH_4 fluxes largely determined the landscape-level CH_4 emissions (Fig. 14). The average annual C uptake of the landscape was -274 ± 169 t C of which 20 % (55 ± 16 t C) was released back to the atmosphere by the lakes (Fig. 14).

The studied landscape consisted of roughly and equal area of pine forest, pine bog, open peatland and lakes (Table 1). Aurela et al. (2015) estimated an annual landscape-level CO_2 balance of -5 g C m^{-2} for a 1963 km^2 area in Pallas in north-western Finland that was comprised of 71 % pine forest, 12 % open wetland, 6 % water surfaces and 2 % treeless fell tops. Within this area, the 105 km^2 Lake Pallasjärvi catchment that included less forests and peatlands, but more lake and fell area, the annual landscape-level CO_2 balance was estimated to be 15 g C m^{-2}. The annual CO_2 uptake in Pallas was lower than in Kaamanen in spite of the much larger proportion of forests. In a study temporally overlapping our study, Chi et al. (2020) reported landscape-level C balances for a typical northern boreal forest landscape in Svartberget, Sweden, where forests covered 87 % of the area; the annual landscape-level CO_2 balance was -37 g C m^{-2} in October 2016 – September 2017 and -108 g C m^{-2} in October 2017 – September 2018. The latter year showed a drought response similar to Kaamanen: a higher annual CO_2 uptake was observed in the forest, while the mire ecosystem (9 % of the area) turned from an annual CO_2 sink to source. The annual CO_2 balances of Svartberget were comparable to Kaamanen, whose pine forest had an annual CO_2 balance of -78 and -119 g C m^{-2} during the first and second study year (Fig. 8d). In a synthesis by Virkkala et al. (2021), the mean annual NEE of 41 boreal biomes was on average -46 g C m^{-2} (uplands -47 g C m^{-2} and wetlands -38 g C m^{-2}); i.e. the CO_2 sink was lower in uplands and larger in wetlands than the mean landscape-scale sink in Kaamanen. These results show that there is large spatial and temporal variation in C exchange among boreal landscapes, but a major part of this derives from the ecosystem composition.

The temporal variation of the landscape-level CO_2 flux (Fig. 13) obviously depended on the flux variation of individual ecosystems. However, different ecosystems showed different environmental responses, and during the two study years there were four periods the ecosystem-specific fluxes deviated from each other and that were reflected in the landscape-level C balance. First, the warmer-than-average early growing season in 2018 increased the CO_2 uptake of the fen ecosystem (Fig. 9a)

https://doi.org/10.5194/bg-2022-69
Preprint. Discussion started: 6 April 2022

and probably also the pine bog fluxes (Figs. 11a, 12a), or conversely the colder-than-average early growing season 2017 led to lower CO_2 uptake by these ecosystems. However, equally large variation in the early growing season CO_2 uptake was not observed in the pine forest fluxes as the evergreen pine forest phenology differs from the largely deciduous mire phenology. Second, the rainy peak growing season 2017 increased the ER of pine forest ecosystem compared to the same period the next year, which decreased the net CO_2 uptake (Figs. 8, A1). This was also reflected in the estimated pine bog fluxes (Figs. 11, 12), but not observed at the fen due to the inherently different water balance between uplands and peatlands. Third, the drought period in summer 2018 decreased CO_2 uptake in both pine forest and fen ecosystems (Figs. 8b, 9b), and the pine bogs likely showed similar response. Finally, the cold spell in autumn 2018 reduced ER causing the forest to revert to a CO_2 sink (Fig. 8), but a similar effect was not observed for the fen. However, the effect of the cold spell was sufficiently strong to be discernible in the modelled pine bog ER fluxes (Figs. 11, 12).

As the pine forest and pine bog CH_4 fluxes used for upscaling were adopted from literature (Dinsmore et al., 2017; Bubier et al., 2005), only the fen and lake ecosystem CH_4 fluxes affect the annual variation in the upscaled landscape-level fluxes. The CH_4 emissions from the fen decreased due to the drought in 2018 (Fig. 9e), thus decreasing the annual emissions compared to the first study year (Table A5). However, as the emissions from lakes increased due to a longer ice-free period in the second year (Table 6), there was only a minor difference in the annual landscape-level CH_4 balance (Fig. 13f, Table A5).

During the two study years, the meteorological conditions were not optimal for C sequestration, as indicated by the lower fen ecosystem CO_2 sink than in some previous years (Aurela et al., 2007). Thus, the landscape-level CO_2 uptake would probably be higher in more optimal conditions. However, the conditions favouring C sequestration differ between ecosystems, as all terrestrial ecosystems are likely to sequester more CO_2 during longer growing seasons, but mires can simultaneously emit more CH_4, and lakes emit more both CO_2 and CH_4.

For estimating the relative radiative impact of the CO_2 and CH_4 exchanges in Kaamanen, the CH_4 flux was translated to CO_2-equivalent flux by multiplying it by the Sustained Global Warming Potential (SGWP) coefficient (Neubauer and Megonigal, 2015; Neubauer, 2021). If the CO_2 and CH_4 observed during the two study years continued for the next 500 yr (SGWP = 14 g CO_2-eq./g CH_4), the net CO_2-equivalent flux of the fen would be positive. However, in longer time scales the fen will eventually have a negative radiative balance even with a low annual CO_2 uptake. In addition to the time-dependent contribution of fens, the annual net CO_2-equivalent flux of the landscape was affected by uptake of both CO_2 and CH_4 by forests, i.e. a systematically negative CO_2-equivalent flux, and emissions of both CO_2 and CH_4 from lakes, i.e. a systematically positive CO_2-equivalent flux. Assuming the present-day fluxes for each ecosystem, upscaling suggests that the net CO_2-equivalent flux of the landscape would be initially positive but turn negative soon after 100 yr (SGWP = 45 g CO_2-eq./g CH_4).

https://doi.org/10.5194/bg-2022-69
Preprint. Discussion started: 6 April 2022

Biogeosciences
Discussions

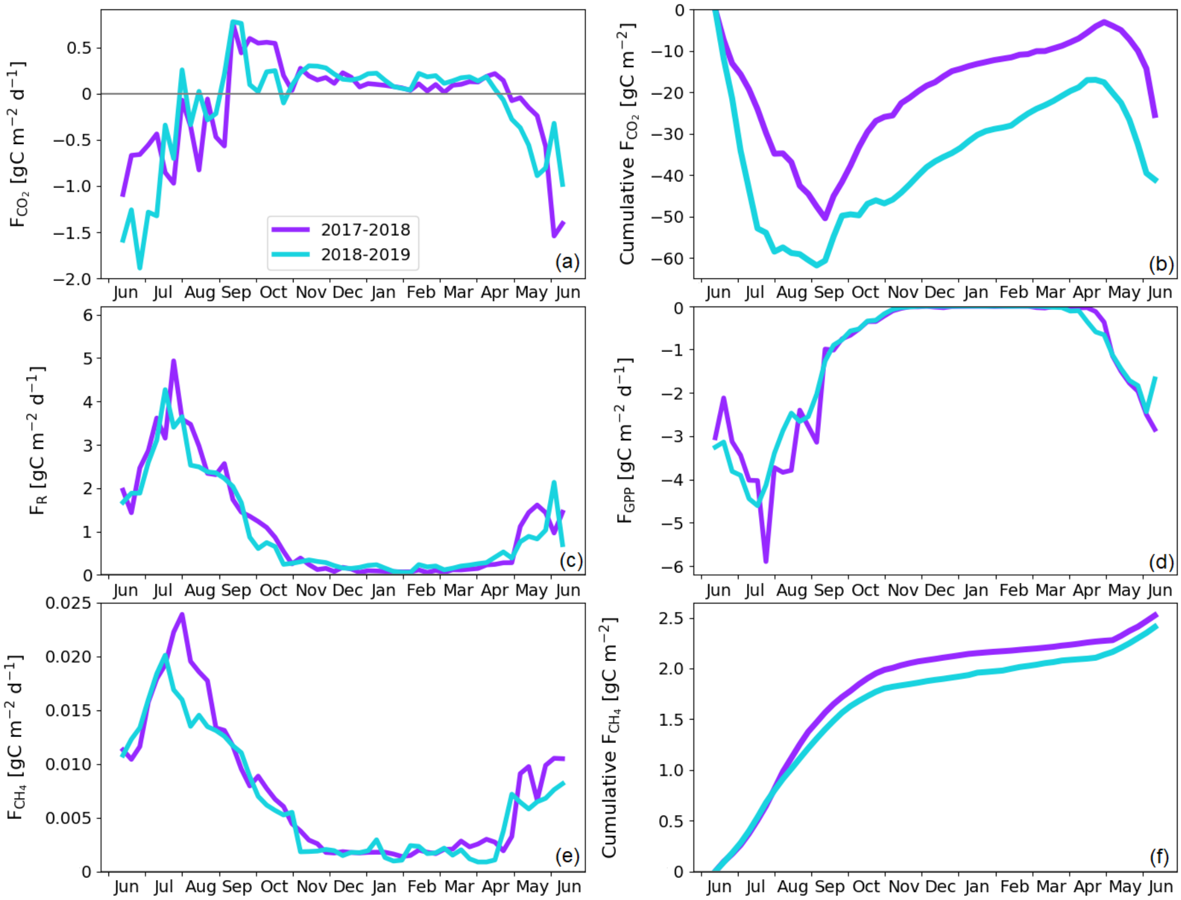

Figure 13. Landscape-level fluxes. Weekly averaged CO_2 (a), ER (c), GPP (d) and CH_4 (e) flux, and cumulative CO_2 (b) and CH_4 (f) flux.

https://doi.org/10.5194/bg-2022-69
Preprint. Discussion started: 6 April 2022

Biogeosciences
Discussions
Open Access
EGU

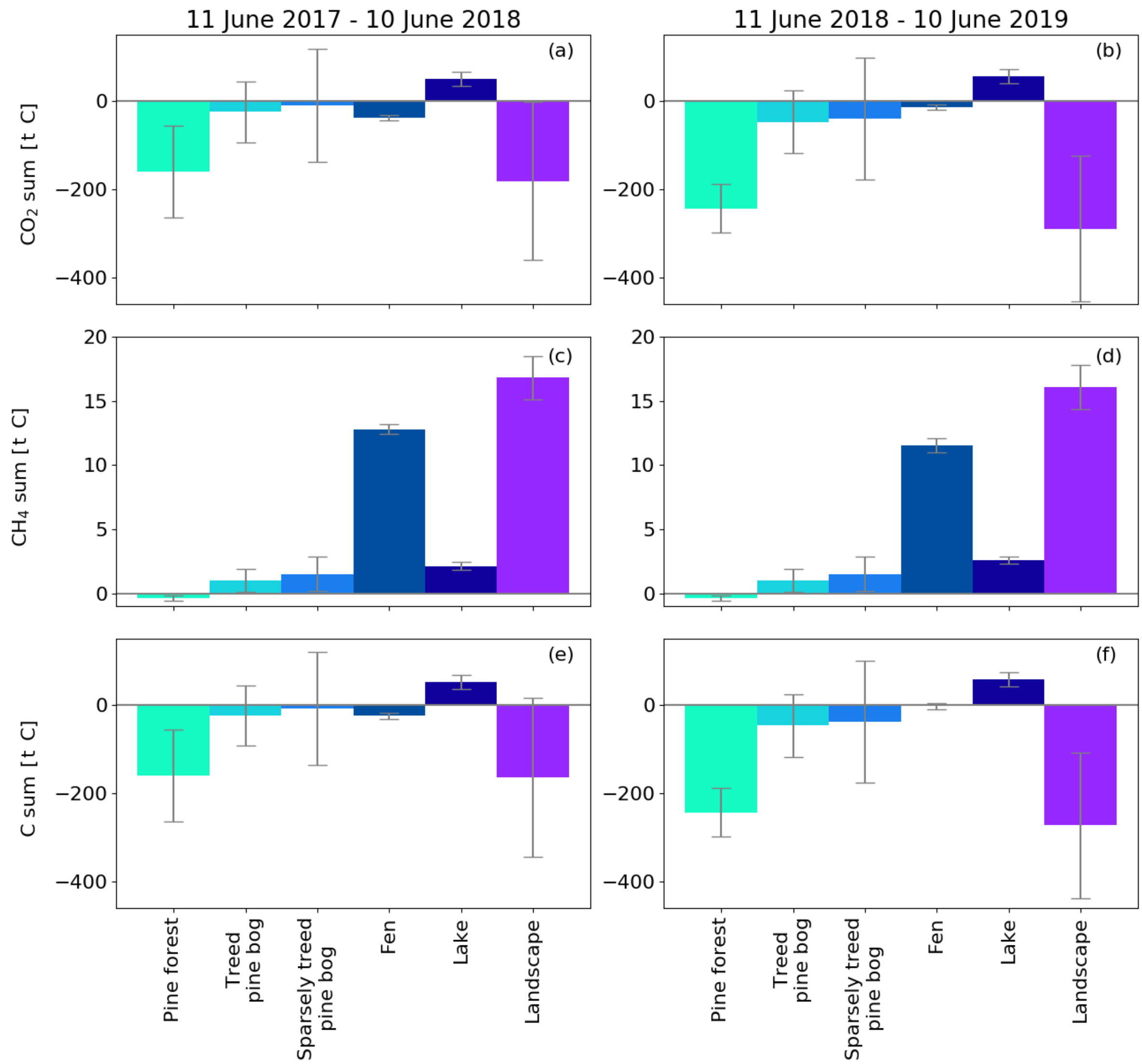

655 **Figure 14.** Annual CO_2, CH_4 and C flux sums for different ecosystems and the landscape (Fig. 1) scaled with the corresponding area. The CH_4 flux estimate for forest is from Dinsmore et al. (2017) and for pine bog from Bubier et al. (2005). The error bars denote the 95 % confidence interval.

4 Conclusions

We estimated the ecosystem-atmosphere exchange of CO_2 and CH_4 for the main ecosystems in a subarctic landscape during
660 two full years. The 7 km^2 study area consisted of pine forest, open peatland, two pine bog ecosystems and two lake types. For the terrestrial ecosystems, C exchange was most sensitive to changes in temperature and moisture conditions, while on the lake it depended on the amount of available carbon in sediment and the length of the ice-free period.

https://doi.org/10.5194/bg-2022-69
Preprint. Discussion started: 6 April 2022

The lakes in the study area released 20 % of the C that was sequestered by the landscape during the study period, and there was a sixfold difference in the CO_2 emissions between organic- and mineral-sediment lakes. Thus, more measurements are needed to determine the role of lake emission variability. Similarly, the CH_4 fluxes were much greater from the organic sediment lake, but the overall impact of lake fluxes on the landscape-scale was smaller than for CO_2. Obviously, the great difference in the observed C fluxes between the lake types should be considered when estimating regional-scale fluxes in a heterogeneous environment such as a northern boreal landscape.

There were four periods when the C fluxes of the terrestrial ecosystems were clearly different between the two study years due to meteorological conditions. In the pine forest, the CO_2 fluxes were affected by the rainy weather in summer 2017, as the high ER rates decreased the CO_2 uptake. The warmer-than-average early growing season in 2018 advanced the plant growth at the fen thus increasing the ecosystem CO_2 uptake. All terrestrial ecosystems were affected by a short but severe drought event in July 2018, which decreased the GPP rates and thus CO_2 uptake. However, both the onset of drought effect and the recovery from drought occurred more rapidly at the fen than in the pine forest. Additionally, during the drought the CH_4 emissions from the fen decreased due to water level drawdown and possibly also due to decreased plant root carbon input. Later, a cold spell in autumn 2018 reduced ER rates in the pine forest ecosystem. The CO_2 flux responses to changing environmental conditions were reflected in the landscape-level CO_2 fluxes, even though only the short and severe drought event affected the CO_2 fluxes of all terrestrial ecosystems similarly. For this reason, none of the ecosystems alone controlled the changes in the landscape-level CO_2 exchange. In contrast to the CO_2 fluxes, it appears that the landscape-level CH_4 flux and its variation can almost entirely be estimated based on the fen data.

Both study years had periods of nonoptimal C sequestration conditions, but still the landscape remained as a CO_2 sink, which indicates that the multitude of ecosystems contribute positively the landscape resilience.

https://doi.org/10.5194/bg-2022-69
Preprint. Discussion started: 6 April 2022

Biogeosciences Discussions
Open Access EGU

Appendix A: Ancillary environmental information, flux and statistical tests

Table A1. Ground layer biomass and leaf area index (mean ± standard deviation) and the number of field measurement points.

Ground layer	Biomass [g dry matter m^{-2}]				Leaf area index [m^{-2} m^{-2}]			n
Land cover class	Shrubs	Forbs and graminoids	Mosses and lichens	Total	Shrubs	Forbs and graminoids	Total	
Pine forest	144.1 ± 73.0	3.2 ± 7.8	398.1 ± 200.7	545.4 ± 189.5	0.39 ± 0.15	0.02 ± 0.04	0.41 ± 0.17	75
Pine bog	284.9 ± 225.6	38.2 ± 30.2	398.4 ± 172.9	721.6 ± 324.5	0.51 ± 0.22	0.22 ± 0.16	0.73 ± 0.25	36
Fen	149.4 ± 90.9	69.6 ± 36.9	146.7 ± 169.1	365.6 ± 231.2	0.21 ± 0.10	0.37 ± 0.19	0.59 ± 0.21	223
String top [a]	247.5 ± 147.4	39.5 ± 29.9	261.8 ± 263.7	548.8 ± 318.8	0.50 ± 0.20	0.21 ± 0.14	0.71 ± 0.19	49

[a] String top CO_2 fluxes were used in pine bog flux estimation for the ground layer flux part, as the two ground layers resemble one another.

Table A2. Average tree height (mean ± standard deviation) and the number of field measurement points.

Ecosystem	Average tree height [m]	n
Pine forest	7.7 ± 2.0	43
Pine bog	4.9 ± 2.0	17

Table A3. Soil and peat properties (mean ± standard deviation) for pine forest, pine bog and fen ecosystems. Except the pine forest organic layer, pH was always measured at 30 cm depth. In pine bog and fen ecosystems, bulk density, C and N content and C:N ratio are the mean of 0–5 and 15–20 cm peat layers.

Ecosystem	pH	Bulk density [g cm^{-3}]	Soil C content [mg cm^{-3}]	Soil N content [mg cm^{-3}]	C:N ratio	No. of sample plots
Pine forest	6.0 ± 0.4					11
Organic layer	4.6 ± 0.2	0.136 ± 0.101	52.9 ± 44.9	1.2 ± 0.9	43.5 ± 8.4	
Eluvial layer		1.037 ± 0.265	20.6 ± 11.9	0.5 ± 0.3	45.7 ± 11.2	
Illuvial layer top		1.219 ± 0.110	16.5 ± 10.4	0.5 ± 0.4	36.4 ± 9.3	
Illuvial layer bottom		1.337 ± 0.145	5.0 ± 4.1	0.2 ± 0.2	43.8 ± 40.1	
50 cm below organic layer		1.511 ± 0.124	2.1 ± 3.3	0.1 ± 0.2	42.4 ± 30.6	
100 cm below organic layer		1.588 ± 0.100	1.1 ± 0.9	0.01 ± 0.02	256 ± 506	
Pine bog	5.0 ± 0.3	0.146 ± 0.246	43.8 ± 29.6	1.2 ± 1.1	44.0 ± 11.8	8
Fen						
String top	4.6 ± 0.4	0.095 ± 0.030	50.9 ± 15.9	1.5 ± 0.8	38.9 ± 10.5	20
String margin	5.7 ± 0.5	0.094 ± 0.046	44.7 ± 21.5	2.5 ± 1.9	24.3 ± 13.0	16
Trichophorum tussock	5.9 ± 0.2	0.133 ± 0.042	57.2 ± 11.3	3.4 ± 0.8	17.1 ± 1.8	18
Flark	5.8 ± 0.2	0.098 ± 0.017	44.2 ± 8.6	2.7 ± 0.6	16.5 ± 2.2	18

https://doi.org/10.5194/bg-2022-69
Preprint. Discussion started: 6 April 2022

Table A4. Tree biomass and leaf area index derived from field and remote sensing measurements.

Ecosystem	Tree biomass [g dry matter m^{-2}]	Tree leaf area index [m^{-2} m^{-2}]
Pine forest	3165	1.97
Treed pine bog	1649	1.02
Sparsely treed pine bog	514	0.32

Table A5. Annual CO_2, CH_4 and C flux balances of the five ecosystems and landscape. The lake flux balances of the second year include scaled estimates using the previous year's measurements on the organic sediment lake. Statistically significant differences between 2017 and 2018 are indicated with an asterisk (Z test, **: $p < 0.05$, *: $p < 0.10$ and ¨: $p < 0.20$).

	11th June 2017 – 10th June 2018	11th June 2018 – 10th June 2019	Difference
CO_2 balance [g C m^{-2}]			
Pine forest	-78.3 ± 50.8	-118.9 ± 26.8	-40.6 ¨
Treed pine bog	-39.1 ± 107.6	-75.0 ± 111.2	-35.9
Sparsely treed pine bog	-9.8 ± 135.4	-42.1 ± 145.3	-32.3
Fen	-20.6 ± 3.6	-7.6 ± 3.7	13.0 **
Lakes	35.6 ± 11.2	(39.0 ± 11.3)	
Landscape	-25.9 ± 65.7	-41.3 ± 64.9	-15.4
CH_4 balance [g C m^{-2}]			
Pine forest	-0.2 ± <0.1 [a]	-0.2 ± <0.1 [a]	
Pine bog	1.6 ± 1.4 [b]	1.6 ± 1.4 [b]	
Fen	7.0 ± 0.2	6.3 ± 0.3	-0.7 **
Lakes	1.5 ± 0.2	(1.8 ± 0.2)	
Landscape	2.4 ± 0.7	2.3 ± 0.7	-0.1
C balance [g C m^{-2}]			
Pine forest	-78.5 ± 50.8	-119.1 ± 26.8	-40.6 ¨
Treed pine bog	-37.5 ± 107.6	-73.4 ± 111.2	-35.9
Sparsely treed pine bog	-8.2 ± 135.4	-40.5 ± 145.3	-32.3
Fen	-13.6 ± 3.6	-1.3 ± 3.7	12.3 **
Lakes	37.1 ± 11.2	(40.8 ± 11.3)	
Landscape	-23.5 ± 65.7	-39.0 ± 64.9	-15.5

[a] From Dinsmore et al. (2017).

[b] From Bubier et al. (2005).

https://doi.org/10.5194/bg-2022-69
Preprint. Discussion started: 6 April 2022

Table A6: Monthly ER, GPP, NEE and CH_4 flux sums. Statistically significant differences between 2017 and 2018 are indicated with an asterisk (Z test, **: $p < 0.05$, *: $p < 0.10$ and ¨: $p < 0.20$).

	ER [g C m⁻²]			GPP [g C m⁻²]			NEE [g C m⁻²]			CH_4 exchange [g C m⁻²]		
Pine forest	2017	2018	Change	2017	2018	Change	2017	2018	Change	2017	2018	Change
June (11-30)	72.8 ± 22.2	59.7 ± 15.4	-13.1	116.8 ± 29.0	117.7 ± 26.7	0.9	-44.4 ± 36.6	-57.5 ± 30.8	-13.1			
July	240.3 ± 70.9	186.4 ± 37.5	-53.9 ¨	253.3 ± 72.4	219.6 ± 48.4	-33.7	-11.8 ± 101.4	-32.4 ± 61.2	-20.6			
August	173.8 ± 37.5	138.0 ± 27.0	-35.8 ¨	182.6 ± 42.7	139.8 ± 37.9	-42.8 ¨	-9.0 ± 56.8	-1.2 ± 46.5	7.8			
September	106.5 ± 58.3	88.0 ± 17.5	-18.5	96.7 ± 79.5	79.4 ± 40.5	-17.3	10.8 ± 98.5	9.1 ± 44.2	-1.6			
October	43.6 ± 40.5	25.0 ± 10.5	-18.6	31.7 ± 36.5	31.6 ± 7.3	-0.1	12.7 ± 54.5	-7.8 ± 12.7	-20.4			
Treed pine bog	2017	2018	Change	2017	2018	Change	2017	2018	Change	2017	2018	Change
June (11-30)	64.7 ± 23.1	48.6 ± 13.5	-16.0	86.8 ± 21.8	96.6 ± 21.1	9.8	-22.4 ± 31.7	-47.7 ± 25.0	-25.3			
July	185.5 ± 65.7	151.1 ± 43.8	-34.4	197.9 ± 58.2	191.5 ± 46.3	-6.5	-11.8 ± 87.8	-40.0 ± 63.7	-28.1			
August	131.6 ± 28.8	112.5 ± 31.8	-19.1	151.4 ± 33.0	118.1 ± 31.6	-33.4 ¨	-19.9 ± 43.8	-5.3 ± 44.9	14.7			
September	77.9 ± 42.3	75.5 ± 13.3	-2.4	71.5 ± 57.4	59.9 ± 29.5	-11.6	6.9 ± 71.3	15.9 ± 32.3	9.0			
October	34.4 ± 29.2	20.9 ± 7.6	-13.5	19.6 ± 26.3	19.6 ± 5.4	0.0	15.2 ± 39.3	0.8 ± 9.3	-14.4			
Sparsely treed pine bog	2017	2018	Change	2017	2018	Change	2017	2018	Change	2017	2018	Change
June (11-30)	58.6 ± 23.5	40.4 ± 11.7	-18.2 ¨	64.3 ± 14.0	80.8 ± 15.5	16.5 ¨	-5.9 ± 27.3	-40.3 ± 19.4	-34.5 **			
July	144.3 ± 60.9	124.6 ± 47.4	-19.7	156.4 ± 44.4	170.3 ± 44.2	13.9	-11.9 ± 75.4	-45.6 ± 64.8	-33.7			
August	99.9 ± 19.7	93.4 ± 34.7	-6.6	128.1 ± 23.2	101.8 ± 25.8	-26.3 ¨	-28.2 ± 30.4	-8.3 ± 43.2	19.8			
September	56.5 ± 24.0	66.1 ± 8.8	9.7	52.6 ± 32.0	45.3 ± 17.0	-7.4	4.0 ± 40.0	20.9 ± 19.2	17.0			
October	27.6 ± 16.3	17.9 ± 4.4	-9.6	10.6 ± 14.6	10.6 ± 3.3	0.0	17.1 ± 21.9	7.2 ± 5.5	-9.9			
Fen	2017	2018	Change	2017	2018	Change	2017	2018	Change	2017	2018	Change
June (11-30)	22.8 ± 5.1	28.2 ± 7.0	5.4	27.6 ± 3.9	49.2 ± 7.3	21.5 **	-4.8 ± 6.4	-21.0 ± 10.1	-16.2 **	0.56 ± 0.02	0.66 ± 0.03	0.09 **
July	68.2 ± 14.9	71.5 ± 14.2	3.3	119.3 ± 14.8	107.2 ± 18.2	-12.0	-51.0 ± 21.1	-35.7 ± 23.1	15.3	1.83 ± 0.03	1.62 ± 0.04	-0.21 **
August	68.1 ± 15.5	61.4 ± 15.8	-6.7	86.8 ± 16.3	71.4 ± 12.3	-15.3 ¨	-18.7 ± 22.5	-10.0 ± 20.0	8.7	1.78 ± 0.06	1.20 ± 0.05	-0.58 **
September	36.3 ± 6.2	35.6 ± 17.2	-0.7	25.6 ± 8.3	20.8 ± 12.5	-4.8	10.7 ± 10.3	14.7 ± 21.3	4.1	0.85 ± 0.02	0.79 ± 0.03	-0.06 **
October	16.7 ± 6.2	13.2 ± 3.7	-3.5	4.7 ± 17.2	2.8 ± 6.8	-2.0	11.9 ± 18.3	10.4 ± 7.7	-1.5	0.46 ± 0.01	0.30 ± 0.04	-0.15 **
Lake	2017	2018 [a]	Change	2017	2018	Change	2017	2018 [a]	Change	2017	2018 [a]	Change
June (11-30)	4.6 ± 2.0	(5.3 ± 2.1)					4.6 ± 2.0	(5.3 ± 2.1)		0.18 ± 0.03	(0.18 ± 0.06)	
July	6.5 ± 3.0	(5.8 ± 2.3)					6.5 ± 3.0	(5.8 ± 2.3)		0.30 ± 0.17	(0.34 ± 0.04)	
August	5.9 ± 2.3	(5.8 ± 2.6)					5.9 ± 2.3	(5.8 ± 2.6)		0.28 ± 0.09	(0.34 ± 0.13)	
September	6.7 ± 3.5	(6.8 ± 2.8)					6.7 ± 3.5	(6.8 ± 2.8)		0.23 ± 0.04	(0.38 ± 0.08)	
October	6.1 ± 2.3	(6.1 ± 2.3)					6.1 ± 2.3	(6.1 ± 2.3)		0.25 ± 0.02	(0.25 ± 0.02)	
Landscape	2017	2018 [a]	Change	2017	2018	Change	2017	2018 [a]	Change	2017	2018 [a]	Change
June (11-30)	41.9 ± 16.8	35.7 ± 11.0	-6.2	57.9 ± 18.1	66.9 ± 17.4	9.0	-16.1 ± 24.8	-30.9 ± 20.6	-14.8	0.18 ± 0.02	0.21 ± 0.03	0.02
July	125.6 ± 50.0	104.8 ± 31.2	-20.8	144.2 ± 47.2	132.5 ± 35.6	-11.7	-18.1 ± 68.8	-27.4 ± 47.3	-9.3	0.54 ± 0.08	0.49 ± 0.02	-0.04
August	95.2 ± 24.9	80.4 ± 23.5	-14.8	107.0 ± 28.2	83.9 ± 25.7	-23.1	-11.9 ± 37.7	-3.4 ± 34.8	8.5	0.52 ± 0.05	0.38 ± 0.07	-0.14 **
September	56.6 ± 35.8	52.2 ± 14.2	-4.4	48.6 ± 48.7	40.2 ± 25.7	-8.4	8.5 ± 60.5	12.2 ± 29.3	3.7	0.27 ± 0.02	0.28 ± 0.04	0.02
October	25.2 ± 24.9	16.3 ± 6.8	-8.9	13.7 ± 24.0	13.2 ± 5.7	-0.5	11.7 ± 34.6	2.7 ± 8.9	-9.0	0.17 ± 0.01	0.13 ± 0.02	-0.04 **

[a] Flux estimates of 2018 include organic lake flux measurements from 2017.

https://doi.org/10.5194/bg-2022-69
Preprint. Discussion started: 6 April 2022

Biogeosciences
Discussions
Open Access
EGU

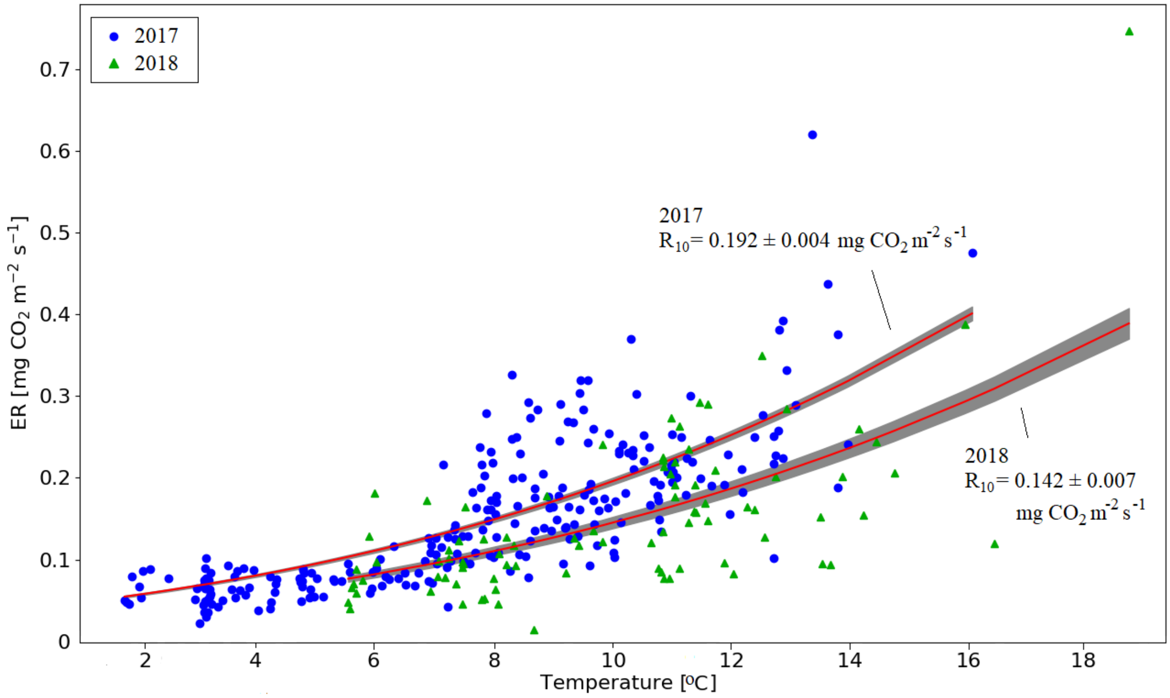

Figure A1. Pine forest ER temperature response curves. Nighttime EC data 15 June – 15 August 2017 and 2018. The lines show the fitted temperature response $\mathrm{ER} = \mathrm{R}_{10} \times e^{\mathrm{E}_0\left(\frac{1}{56.02}-\frac{1}{\mathrm{T}-227.13}\right)}$, with E_0= 400 K^{-1} (Lloyd and Taylor, 1994). The shaded areas indicate the one sigma confidence intervals.

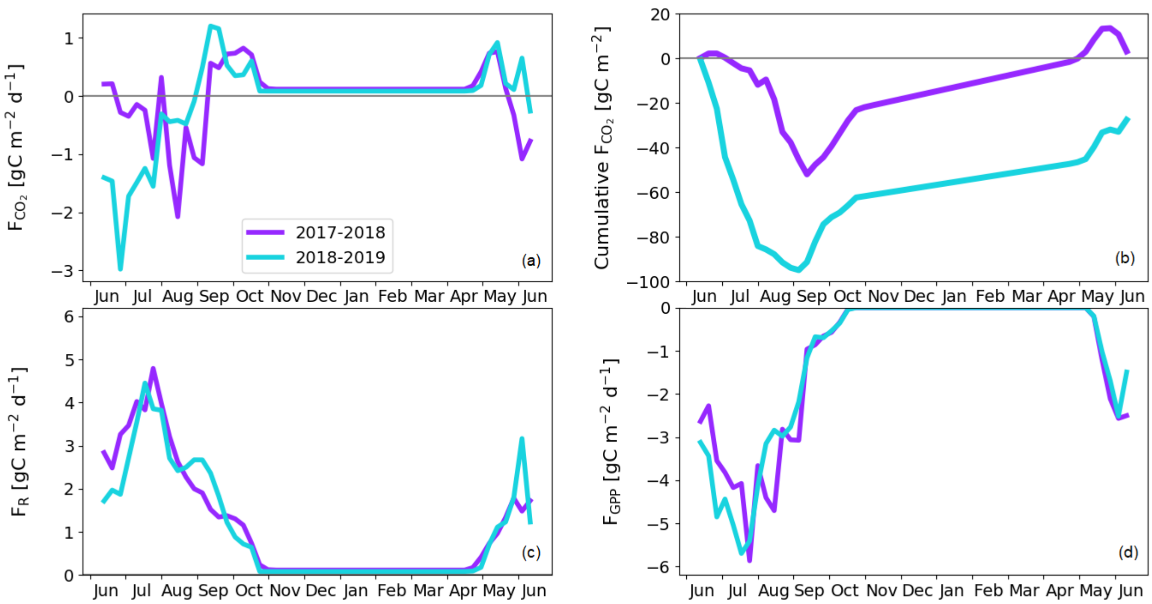

Figure A2. String top fluxes. Weekly averaged (a) and cumulative CO_2 flux (b), and weekly averaged ER (c) and GPP (d) flux, used for estimating pine bog ecosystem fluxes.

https://doi.org/10.5194/bg-2022-69
Preprint. Discussion started: 6 April 2022

Table A7. Average bulk density, C and N content and C:N ratio (± standard deviation) in the top 20 cm of lake sediments.

Lake	Bulk density [g cm^{-3}]	Soil C content of dry mass [%]	Soil N content of dry mass [%]	C:N ratio	No. of core samples
Jänkäjärvi (organic sediment lake)	0.13 ± 0.03	30.3 ± 1.6	1.6 ± 0.1	18.4 ± 1.0	1
Jänkälampi (mineral sediment lake)					
Northern basin	0.91 ± 0.47	5.5 ± 5.4	0.3 ± 0.3	19.9 ± 6.2	4
Southern basin	0.13 ± 0.10	22.6 ± 3.1	1.4 ± 0.4	15.6 ± 2.7	1

Data availability. The measured flux and ancillary meteorological and environmental data are available on Zenodo (https://doi.org/10.5281/zenodo.6334237, last access: 7 March 2022, Heiskanen et al., 2022).

Author contributions. MA, JPT and LH designed the study. Terrestrial ecosystem field flux measurements and maintenance were carried out by LH and MA. Aquatic ecosystem field flux measurements were carried out by LH, MA and SJ. AR, TV and SJ measured and analysed the vegetation and land cover data. JM measured and analysed the soil data. SJ and LH collected the lake sediment data, and SJ and JM took part in the sediment data analysis. AR and TV conducted the linear regression model analysis. HV produced the eddy covariance gap-filling program code. The rest of the data analysis was carried out by LH, JPT and MA. LH wrote the paper with contributions from all co-authors.

Competing interests. The authors declare that they have no conflict of interest.

Acknowledgements. We thank Jani Antila, Holtti Hakonen and Tuuli Lehtosalo for field assistance and Jan Weckström and Maija Heikkilä for granting ancillary lake sediment chemistry data. We thank Tuomas Laurila and Timo Penttilä for expert support on planning the measurement site set-up.

Financial support. This research has been supported by the Academy of Finland (grant no. 296423).

References

Aguadé, D., Poyatos, R., Gómez, M., Oliva, J. and Martínez-Vilalta, J.: The role of defoliation and root rot pathogen infection in driving the mode of drought-related physiological decline in Scots pine (Pinus sylvestris L.), Tree Physiol., 35, 229-242, doi:10.1093/treephys/tpv005, 2015.

Alm, J., Schulman, L., Walden, J., Nykänen, H., Martikainen, P. J., and Silvola, J.: Carbon Balance of a Boreal Bog during a Year with an Exceptionally Dry Summer, Ecology, 80, 161–174, https://doi.org/10.1890/0012-9658(1999)080[0161:CBOABB]2.0.CO;2, 1999.

Aubinet, M., Vesala, T., and Papale, D.: Eddy Covariance: A Practical Guide to Measurement and Data Analysis, Springer Netherlands, Dordrecht, https://doi.org/10.1007/978-94-007-2351-1, 2012.

Aurela, M., Laurila, T., and Tuovinen, J.-P: Seasonal CO_2 balances of a subarctic mire, J. Geophys. Res.-Atmos., 106, 1623–1637, https://doi.org/10.1029/2000JD900481, 2001.

Aurela, M., Laurila, T., and Tuovinen, J.-P.: Annual CO2 balance of a subarctic fen in northern Europe: Importance of the wintertime efflux, J. Geophys. Res.-Atmos., 107, 4607, https://doi.org/10.1029/2002JD002055, 2002.

Aurela, M., Laurila, T., and Tuovinen, J.-P.: The timing of snow melt controls the annual CO_2 balance in a subarctic fen, Geophys. Res. Lett., 31, L16119, https://doi.org/10.1029/2004GL020315, 2004.

https://doi.org/10.5194/bg-2022-69
Preprint. Discussion started: 6 April 2022

Biogeosciences Discussions

Aurela, M., Riutta, T., Laurila, T., Tuovinen, J.-P., Vesala, T., Tuittila, E., Rinne, J., Haapanala, S., and Laine, J.: CO_2 exchange of a sedge fen in southern Finland-the impact of a drought period, Tellus B, 59, 826–837, https://doi.org/10.1111/j.1600-0889.2007.00309.x, 2007.

Aurela M., Lohila A., Tuovinen J.-P., Hatakka J., Penttilä T. and Laurila T.: Carbon dioxide and energy flux measurements in four northern-boreal ecosystems at Pallas. Boreal Env. Res. 20: 455–473, 2015.

Barton, K.: MuMIn: Multi-Model Inference. R package version 1.43.17. https://CRAN.R-project.org/package=MuMIn (last access 1 October 2021), 2020.

Bastviken, D., Cole, J., Pace, M. and Tranvik, L.: Methane emissions from lakes: Dependence of lake characteristics, two regional assessments, and a global estimate, Global Biogeochem. Cycles, 18, GB4009, doi:10.1029/2004GB002238, 2004.

Bond-Lamberty, B., Peckham, S. D., Ahl, D. E., and Gower, S. T.: Fire as the dominant driver of central Canadian boreal forest carbon balance. Nature, 450, 89–92. https://doi.org/10.1038/nature06272, 2007.

Breiman, L.: Random forests. *Machine learning*, *45*(1), 5-32, 2001.

Bubier, J. L., Crill, P. M., Moore, T. R., Savage, K., and Varner, R. K.: Seasonal patterns and controls on net ecosystem CO_2 exchange in a boreal peatland complex, Global Biogeochem. Cy., 12, 703–714, https://doi.org/10.1029/98GB02426, 1998.

Bubier, J., Moore, T., Savage, K. and Crill, P.: A comparison of methane flux in a boreal landscape between a dry and a wet year, Global Biogeochem. Cycles, 19, GB1023-n/a, doi:10.1029/2004GB002351, 2005.

Büker, P., Morrissey, T., Briolat, A., Falk, R., Simpson, D., Tuovinen, J.-P., Alonso, R., Barth, S., Baumgarten, M., Grulke, N., Karlsson, P. E., King, J., Lagergren, F., Matyssek, R., Nunn, A., Ogaya, R., Penuelas, J., Rhea, L., Schaub, M., Uddling, J., Werner, W. and Emberson, L. D.: DO3SE modelling of soil moisture to determine ozone flux to forest trees, Atmospheric chemistry and physics, 12, 5537-5562, doi:10.5194/acp-12-5537-2012, 2012.

Chapin, F. S., Matson, P. A., and Vitousek, P.: Principles of Terrestrial Ecosystem Ecology (Second Edition), Springer, https://doi.org/10.1007/978-1-4419-9504-9, 2011.

Chi, J., Nilsson, M. B., Laudon, H., Lindroth, A., Wallerman, J., Fransson, J. E. S., Kljun, N., Lundmark, T., Ottosson Löfvenius, M. and Peichl, M.: The Net Landscape Carbon Balance—Integrating terrestrial and aquatic carbon fluxes in a managed boreal forest landscape in Sweden, Global Change Biol., 26, 2353-2367, doi:10.1111/gcb.14983, 2020.

Cole, J. J., Prairie, Y. T., Caraco, N. F., McDowell, W. H., Tranvik, L. J., Striegl, R. G., Duarte, C. M., Kortelainen, P., Downing, J. A., Middelburg, J. J., and Melack, J.: Plumbing the global carbon cycle: Integrating inland waters into the terrestrial carbon budget. Ecosystems, 10(1), 171-184. https://doi.org/10.1007/s10021-006-9013-8, 2007.

Denfeld, B. A., Lupon, A., Sponseller, R. A., Laudon, H. and Karlsson, J.: Heterogeneous CO_2 and CH_4 patterns across space and time in a small boreal lake, Inland Waters, 10:3, 348-359, DOI: 10.1080/20442041.2020.1787765, 2020.

https://doi.org/10.5194/bg-2022-69
Preprint. Discussion started: 6 April 2022

Deppe, M., Knorr, K-H., McKnight, D. M., and Blodau, C.: Effects of short-term drying and irrigation on CO_2 and CH_4 production and emission from mesocosms of a northern bog and an alpine fen, Biogeochemistry, 100, 89–103, https://doi.org/10.1007/s10533-010-9406-9, 2010.

Dinsmore, K. J., Drewer, J., Levy, P. E., George, C., Lohila, A., Aurela, M. and Skiba, U. M.: Growing season CH_4 and N_2O fluxes from a subarctic landscape in northern Finland; from chamber to landscape scale. Biogeosciences, 14(4), 799–815. https://doi.org/10.5194/bg-14-799-2017, 2017.

Du, Y., Wang, Y., Su, F., Jiang, J., Wang, C., Yu, M. and Yan, J.: The response of soil respiration to precipitation change is asymmetric and differs between grasslands and forests, Global Change Biol., 26, 6015-6024, doi:10.1111/gcb.15270, 2020.

Foken, T. and Wichura, B.: Tools for quality assessment of surface-based flux measurements, Agr. Forest Meteorol., 78, 83–105, https://doi.org/10.1016/0168-1923(95)02248-1, 1996.

Fronzek, S., Carter, T., Räisänen, J., Ruokolainen, L., Luoto, M.: Applying probabilistic projections of climate change with impact models: A case study for sub-arctic palsa mires in Fennoscandia. Climatic Change. 99. 515-534. https://doi.org/10.1007/s10584-009-9679-y, 2010.

Gao, Y., Markkanen, T., Aurela, M., Mammarella, I., Thum, T., Tsuruta, A., Yang, H. and Aalto, T.: Response of water use efficiency to summer drought in a boreal Scots pine forest in Finland, Biogeosciences, 14, 4409–4422, https://doi.org/10.5194/bg-14-4409-2017, 2017.

Guo, M., Zhuang, Q., Tan, Z., Shurpali, N., Juutinen, S., Kortelainen, P., Martikainen, P. J.: Rising methane emissions from boreal lakes due to increasing ice-free days, Environ. Res. Lett., 15, 064008, https://doi.org/10.1088/1748-9326/ab8254

Hadden, D. and Grelle, A.: Net CO_2 emissions from a primary boreo-nemoral forest over a 10 year period. Forest Ecology and Management, 398, 164–173. https://doi.org/10.1016/j.foreco.2017.05.008, 2017.

Hargreaves, K. J., Fowler, D., Pitcairn, C. E. R., and Aurela, M.: Annual methane emission from Finnish mires estimated from eddy covariance campaign measurements, Theor. Appl. Climatol., 70, 203–213, https://doi.org/10.1007/s007040170015, 2001.

Heiskanen, L., Tuovinen, J.-P., Räsänen, A., Virtanen, T., Juutinen, S., Lohila, A., Penttilä, T., Linkosalmi, M., Mikola, J., Laurila, T., and Aurela, M.: Carbon dioxide and methane exchange of a patterned subarctic fen during two contrasting growing seasons, Biogeosciences, 18, 873–896, https://doi.org/10.5194/bg-18-873-2021, 2021.

Heiskanen, L., Tuovinen, J-P., Räsänen, A., Virtanen, T., Juutinen, S., Vekuri, H., Lohila, A., Mikola, J., and Aurela, M.: Meteorological responses of carbon dioxide and methane fluxes in the terrestrial and aquatic ecosystems of a subarctic landscape [Data set], Zenodo, https://doi.org/10.5281/zenodo.6334237, 2022.

Jammet, M., Dengel, S., Kettner, E., Parmentier, F.-J. W., Wik, M., Crill, P., and Friborg, T.: Year-round CH_4 and CO_2 flux dynamics in two contrasting freshwater ecosystems of the subarctic, Biogeosciences, 14, 5189–5216, https://doi.org/10.5194/bg-14-5189-2017, 2017.

Jansen, J., Thornton, B. F., Cortés, A., Snöälv, J., Wik, M., MacIntyre, S., and Crill, P. M.: Drivers of diffusive CH_4 emissions from shallow subarctic lakes on daily to multi-year timescales, Biogeosciences, 17, 1911–1932, https://doi.org/10.5194/bg-17-1911-2020, 2020.

Jones, H. G.: Plants and Microclimate: A Quantitative Approach to Environmental Plant Physiology, Cambridge University Press, West Nyack, https://doi.org/10.1017/CBO9780511845727, 2013.

Juutinen, S., Väliranta, M., Kuutti, V., Laine, A. M., Virtanen, T., Seppä, H., Weckström, J. and Tuittila, E-S.: Short-term and long-term carbon dynamics in a northern peatland-stream-lake continuum: A catchment approach, J.Geophys.Res.Biogeosci., 118, 171-183, doi:10.1002/jgrg.20028, 2013.

Kätterer, T., Reichstein, M., Andrén, O., and Lomander, A.: Temperature dependence of organic matter decomposition: a critical review using literature data analyzed with different models. Biol. Fertil. Soils 27, 258–262, https://doi.org/10.1007/s003740050430, 1998.

Kljun, N., Black, T. A., Griffis, T. J., Barr, A. G., Gaumont-Guay, D., Morgenstern, K., McCaughey, J. H. and Nesic, Z.: Response of net ecosystem productivity of three boreal forest stands to drought. Ecosystems, 10, 1039–1055. https://doi.org/10.1007/s10021-007-9088-x, 2007.

Laurila, T., Soegaard, H., Lloyd, C. R., Aurela, M., Tuovinen, J.-P., and Nordstroem, C.: Seasonal variations of net CO_2 exchange in European Arctic ecosystems, Theor. Appl. Climatol., 70, 183– 201, https://doi.org/10.1007/s007040170014, 2001.

Laurila T., Tuovinen J.-P., Lohila A., Hatakka J., Aurela M., Thum T., Pihlatie M., Rinne J. and Vesala T.: Measuring methane emissions from a landfill using a cost effective micrometeorological method. Geophys. Res. Let. 32: LI9808, https://doi.org/10.1029/2005GLO23462, 2005.

Lehtonen, I. and Pirinen, P.: 2018: An exceptionally warm thermal growing season in Finland, in: FMI's Climate Bulletin: Research Letters, Helsinki, Finnish Meteorological Institute, https://doi.org/10.35614/ISSN-2341-6408-IK-2019-03-RL, 2019a.

Lehtonen, I. and Pirinen, P.: 2018: An exceptionally dry thermal growing season in Finland, in: FMI's Climate Bulletin: Research Letters, Helsinki, Finnish Meteorological Institute, https://doi.org/10.35614/ISSN-2341-6408-IK-2019-04-RL, 2019b.

Le Mer, J. and Roger, P.: Production, oxidation, emission and consumption of methane by soils: A review, European Journal of Soil Biology, 37(1), 25–50, https://doi.org/10.1016/S1164-5563(01)01067-6, 2001.

Liaw, A., and Wiener, M.: Classification and regression by randomForest. *R news*, *2*(3), 18-22, 2002.

Lindroth, A., Lund, M., Nilsson, M., Aurela, M., Christensen, T. R., Laurila, T., Rinne, J., Riutta, T., Sagerfors, J., SträM, L., Tuovinen, J. and Vesala, T.: Environmental controls on the CO_2 exchange in north European mires, 59, 812-825, doi:10.1111/j.1600-0889.2007.00310.x, 2007.

https://doi.org/10.5194/bg-2022-69
Preprint. Discussion started: 6 April 2022

Biogeosciences Discussions

Lindroth, A., Lagergren, F., Aurela, M., Bjarnadottir, B., Christensen, T., Dellwik, E., Grelle, A., Ibrom, A., Johansson, T., Lankreijer, H., Launiainen, S., Laurila, T., Mölder, M., Nikinmaa, E., Pilegaard, K., Sigurdsson, B. D., and Vesala, T.: Leaf area index is the principal scaling parameter for both gross photosynthesis and ecosystem respiration of Northern deciduous and coniferous forests. Tellus. Series B, Chemical and Physical Meteorology, 60(2). https://doi.org/10.3402/tellusb.v60i2.16909, 2008.

Lindroth, A., Holst, J., Linderson, M., Aurela, M., Biermann, T., Heliasz, M., Chi, J., Ibrom, A., Kolari, P., Klemedtsson, L., Krasnova, A., Laurila, T., Lehner, I., Lohila, A., Mammarella, I., Mölder, M., Löfvenius, M. O., Peichl, M., Pilegaard, K., Soosar, K., Vesala, T., Vestin, P., Weslien, P. and Nilsson, M.: Effects of drought and meteorological forcing on carbon and water fluxes in Nordic forests during the dry summer of 2018, Philos. Trans. R. Soc. Lond. , B, Biol. Sci., 375, 20190516, doi:10.1098/rstb.2019.0516, 2020.

Lloyd, J. and Taylor, J. A.: On the Temperature Dependence of Soil Respiration, Funct. Ecol., 8, 315–323, https://doi.org/10.2307/2389824, 1994.

Lohila, A., Tuovinen, J.-P., Hatakka, J., Aurela, M., Vuorenmaa, J., Haakana, M. and Laurila, T.: Carbon dioxide and energy fluxes over a northern boreal lake, Boreal Environ. Res., 20, 474-488, ISSN 1797-2469 (online), 2015.

Maanavilja, L., Riutta, T., Aurela, M., Laurila, T., and Tuittila, E-S.: Spatial variation in CO_2 exchange at a northern aapa mire, Biogeochemistry, 104, 325–345, https://doi.org/10.1007/s10533-010-9505-7, 2011.

Martín-Gómez, P., Aguilera, M., Pemán, J., Gil-Pelegrín, E., and Ferrio, J. P.: Contrasting ecophysiological strategies related to drought: the case of a mixed stand of Scots pine (*Pinus sylvestris*) and a submediterranean oak (*Quercus subpyrenaica*), Tree Physiology, Vol. 37, 11, 1478–1492, https://doi.org/10.1093/treephys/tpx101, 2017.

Masson-Delmotte, V., Zhai, P., Pörtner, H.-O., Roberts, D., Skea, J., Shukla, P. R., Pirani, A., Moufouma-Okia, W., Péan, C., Pidcock, R., Connors, S., Matthews, J. B. R., Chen, Y., Zhou, X., Gomis, M. I., Lonnoy, E., Maycock, T., Tignor, M., and Waterfield T.: Global Warming of $1.5^{\circ}C$. An IPCC Special Report on the impacts of global warming of $1.5^{\circ}C$ above pre-industrial levels and related global greenhouse gas emission pathways, in the context of strengthening the global response to the threat of climate change, sustainable development, and efforts to eradicate poverty, World Meteorological Organization, Geneva, Switzerland, 2018.

Matkala, L., Kulmala, L., Kolari, P., Aurela, M., and Bäck, J.: Resilience of subarctic Scots pine and Norway spruce forests to extreme weather events. Agricultural and Forest Meteorology, 296. https://doi.org/10.1016/j.agrformet.2020.108239, 2021.

McElligott, K. M., Seiler, J. R. and Strahm, B. D.: The Impact of Water Content on Sources of Heterotrophic Soil Respiration, Forests, 8, 299, doi:10.3390/f8080299, 2017.

McMillen, R. T.: An eddy correlation technique with extended applicability to non-simple terrain, Bound.-Lay. Meteorol., 43, 231–245, https://doi.org/10.1007/BF00128405, 1988.

Mekonnen, Z. A., Riley, W. J., Berner, L. T., Bouskill, N. J., Torn, M. S., Iwahana, G., Breen, A. L., Myers-Smith, I. H., García Criado, M., Liu, Y., Euskirchen, E. S., Goetz, S. J., Mack, M. C. and Grant, R. F.: Arctic tundra shrubification: a review of mechanisms and impacts on ecosystem carbon balance, Environ. Res. Lett. 16, 053001, https://doi.org/10.1088/1748-9326/abf28b, 2021.

Meyer, N., Welp, G., and Amelung, W.: The temperature sensitivity (Q10) of soil respiration: controlling factors and spatial prediction at regional scale based on environmental soil classes. Global Biogeochem. Cycles 32, 306–323, https://doi.org/10.1002/2017GB005644, 2018.

Montagnani, L., Grünwald, T., Kowalski, A., Mammarella, I., Merbold, L., Metzger, S., Sedlák, P. and Siebicke, L.: Estimating the storage term in eddy covariance measurements: the ICOS methodology, International Agrophysics, 32, 551-567, doi:10.1515/intag-2017-0037, 2018.

Moyano, F. E., Vasilyeva, N., Bouckaert, L., Cook, F., Craine, J., Curiel Yuste, J., Don, A., Epron, D., Formanek, P., Franzluebbers, A., Ilstedt, U., Kätterer, T., Orchard, V., Reichstein, M., Rey, A., Ruamps, L., Subke, J. -., Thomsen, I. K. and Chenu, C.: The moisture response of soil heterotrophic respiration: interaction with soil properties, Biogeosciences, 9, 1173-1182, doi:10.5194/bg-9-1173-2012, 2012.

Muilu-Mäkelä, R., Vuosku, J., Läärä, E., Saarinen, M., Heiskanen, J., Häggman, H. and Sarjala, T.: Water availability influences morphology, mycorrhizal associations, PSII efficiency and polyamine metabolism at early growth phase of Scots pine seedlings, Plant Physiol. Biochem., 88, 70-81, doi:10.1016/j.plaphy.2015.01.009, 2015.

Neubauer, S.C. and Megonigal, J.P.: Moving Beyond Global Warming Potentials to Quantify the Climatic Role of Ecosystems, Ecosystems 18, 1000–1013, https://doi.org/10.1007/s10021-015-9879-4, 2015.

Neubauer, S.C.: Global Warming Potential Is Not an Ecosystem Property, Ecosystems 24, 2079–2089, https://doi.org/10.1007/s10021-021-00631-x, 2021.

Orchard, V. A. and Cook, F. J.: Relationship between soil respiration and soil moisture, Soil Biol. Biochem., Vol. 15, No. 4, pp. 447-453, 1983.

Piilo, S. R., Korhola, A., Heiskanen, L., Tuovinen, J-P., Aurela, M., Juutinen, S., Marttila, H., Saari, M., Tuittila, E-S., Turunen, J., and Väliranta, M. M.: Spatially varying peatland initiation, Holocene development and estimated radiative forcing within a subarctic fen, Quaternary Sci. Rev., 248, 106596, https://doi.org/10.1016/j.quascirev.2020.106596, 2020.

Pirinen, P., Simola, H., Aalto, J., Kaukoranta, J.-P., Karlsson, P., and Ruuhela, R.: Climatological Statistics of Finland 1981–2010., Reports 2012, Finnish Meteorological Institute, ISSN 0782-6079, 2012.

Räsänen, M., Aurela, M., Vakkari, V., Beukes, J. P., Tuovinen, J.-P., Van Zyl, P. G., Josipovic, M., Venter, A. D., Jaars, K., Siebert, S. J., Laurila, T., Rinne, J., and Laakso, L.: Carbon balance of a grazed savanna grassland ecosystem in South Africa, Biogeosciences, 14, 1039–1054, https://doi.org/10.5194/bg-14- 1039-2017, 2017.

Räsänen, A. and Virtanen, T.: Data and resolution requirements in mapping vegetation in spatially heterogeneous landscapes, Remote Sens. Environ., 230, 111207, https://doi.org/10.1016/j.rse.2019.05.026, 2019.

Räsänen, A., Juutinen, S., Tuittila, E-S., Aurela, M. and Virtanen, T.: Comparing ultra-high spatial resolution remote-sensing methods in mapping peatland vegetation, Journal of Vegetation Science, vol. 30, no. 5, pp. 1016-1026. https://doi.org/10.1111/jvs.12769, 2019.

Rasilo, T., Prairie, Y. T. and del Giorgio, P. A.: Large-scale patterns in summer diffusive CH_4 fluxes across boreal lakes, and contribution to diffusive C emissions, Global Change Biol., 21, 1124-1139, doi:10.1111/gcb.12741, 2015.

R Core Team: R: A language and environment for statistical computing. R Foundation for Statistical Computing, Vienna, Austria, available at: https://www.R-project.org (last access: 1 October 2021), 2021.

Repola, J.: Biomass equations for Scots pine and Norway spruce in Finland. Silva Fennica, 43(4), 625-647, ISSN 0037-5330, 2009.

Rinne J., Tuovinen J.-P., Klemedtsson L., Aurela M., Holst J., Lohila A., Weslien P., Vestin P., Łakomiec P., Peichl M., Tuittila E.-S., Heiskanen L., Laurila T., Li X., Alekseychik P., Mammarella I., Ström L., Crill P., and Nilsson M. B.: Effect of the 2018 European drought on methane and carbon dioxide exchange of northern mire ecosystems. Phil. Trans. R. Soc., 375, B37520190517, https://doi.org/10.1098/rstb.2019.0517, 2020.

Sagerfors, J., Lindroth, A., Grelle, A., Klemedtsson, L., Weslien, P. and Nilsson, M.: Annual CO_2 exchange between a nutrient-poor, minerotrophic, boreal mire and the atmosphere, J. Geophys. Res., 113, G01001, doi:10.1029/2006JG000306, 2008.

Sepulveda-Jauregui, A., Walter Anthony, K. M., Martinez-Cruz, K., Greene, S., and Thalasso, F.: Methane and carbon dioxide emissions from 40 lakes along a north–south latitudinal transect in Alaska, Biogeosciences, 12, 3197–3223, https://doi.org/10.5194/bg-12-3197-2015, 2015.

Silfver, T., Heiskanen, L., Aurela, M., Myller, K., Karhu, K., Meyer, N., Tuovinen, J-P., Oksanen, E., Rousi, M. and Mikola, J.: Insect herbivory dampens subarctic birch forest C sink response to warming, Nat. Commun. 11, 2529, https://doi.org/10.1038/s41467-020-16404-4, 2020.

Strack, M. and Waddington, J. M.: Response of peatland carbon dioxide and methane fluxes to a water table drawdown experiment, Global Biogeochem. Cy., 21, GB1007, https://doi.org/10.1029/2006GB002715, 2007.

Thornton, B. F., Wik, M. and Crill, P. M.: Climate-forced changes in available energy and methane bubbling from subarctic lakes, Geophys. Res. Lett., 42, 1936-1942, doi:10.1002/2015GL063189, 2015.

Tranvik, L. J., Downing, J. A., Cotner, J. B., Loiselle, S. A., Striegl, R. G., Ballatore, T. J., Dillon, P., Knoll, L. B., Kutser, T., Larsen, S., Laurion, I., Leech, D. M., McAllister, S. L., McKnight, D. M., Melack, J., Overholt, E., Porter, J. A., Prairie, Y. T., Renwick, W. H., Roland, F., Sherman, B. S., Schindler, D. W., Sobek, S., Tremblay, A., Vanni, M. J., Verschoor, A. M., von Wachenfeldt, E. and Weyhenmeyer, G.: Lakes and Reservoirs as Regulators of Carbon Cycling and Climate, Limnol. Oceanogr., 54, 2298-2314, doi:10.4319/lo.2009.54.6_part_2.2298, 2009.

Venables, W. N. and Ripley, B. D.: Modern Applied Statistics with S, Fourth Edition, Springer, New York, https://doi.org/10.1007/978-0-387-21706-2, 2002.

Vicente-Serrano, S., Begueria, S. and Lopez-Moreno, J.: A Multiscalar Drought Index Sensitive to Global Warming: The Standardized Precipitation Evapotranspiration Index, J. Clim., 23, 1696-1718, doi:10.1175/2009JCLI2909.1, 2010.

https://doi.org/10.5194/bg-2022-69
Preprint. Discussion started: 6 April 2022

Virkkala, A. M., Aalto, J., Rogers, B. M., Tagesson, T., Treat, C. C., Natali, S. M., Watts, J. D., Potter, S., Lehtonen, A., Mauritz, M., Schuur, E. A. G., Kochendorfer, J., Zona, D., Oechel, W., Kobayashi, H., Humphreys, E., Goeckede, M., Iwata, H., Lafleur, P. M., Euskirchen, E. S., Bokhorst, S., Marushchak, M., Martikainen, P. J., Elberling, B., Voigt, C., Biasi, C., Sonnentag, O., Parmentier, F. J. W., Ueyama, M., Celis, G., St.Louis, V.,L., Emmerton, C. A., Peichl, M., Chi, J., Järveoja, J., Nilsson, M. B., Oberbauer, S. F., Torn, M. S., Park, S. J., Dolman, H., Mammarella, I., Chae, N., Poyatos, R., López-Blanco, E., Christensen, T. R., Kwon, M. J., Sachs, T., Holl, D. and Luoto, M.: Statistical upscaling of ecosystem CO_2 fluxes across the terrestrial tundra and boreal domain: Regional patterns and uncertainties, Global Change Biol., 27, 4040-4059, doi:10.1111/gcb.15659, 2021.

Walter, K. M., Zimov, S. A., Chanton, J. P., Verbyla, D. and Chapin, F.S. III: Methane bubbling from Siberian thaw lakes as a positive feedback to climate warming, Nature, 443, 71-75, doi:10.1038/nature05040, 2006.

White, J. R., Shannon, R. D., Weltzin, J. F., Pastor, J., and Bridgham, S. D.: Effects of soil warming and drying on methane cycling in a northern peatland mesocosm study, J. Geophys. Res.- Biogeo., 113, G00A06, https://doi.org/10.1029/2007JG000609, 2008

Wik, M., Crill, P. M., Varner, R. K. and Bastviken, D.: Multiyear measurements of ebullitive methane flux from three subarctic lakes, J.Geophys.Res.Biogeosci., 118, 1307-1321, doi:10.1002/jgrg.20103, 2013.

Wik, M., Johnson, J. E., Crill, P. M., DeStasio, J. P., Erickson, L., Halloran, M. J., Fahnestock, M. F., Crawford, M. K., Phillips, S. C. and Varner, R. K.: Sediment Characteristics and Methane Ebullition in Three Subarctic Lakes, Journal of geophysical research. Biogeosciences, 123, 2399-2411, doi:10.1029/2017JG004298, 2018.